



Homogenized Korteweg–de Vries and Boussinesq models for anisotropic propagation of solitary waves over a structured bathymetry

Kim Pham,¹ Agnès Maurel²  and Amin Chabchoub^{3,4}

¹LMI, ENSTA Paris, Institut Polytechnique de Paris, 91120 Palaiseau, France

²Institut Langevin, ESPCI Paris, CNRS, Université PSL, Sorbonne Université, 1 rue Jussieu, 75005 Paris, France

³Marine Physics and Engineering Unit, Okinawa Institute of Science and Technology, Onna-son, Okinawa 904-0495, Japan

⁴Department of Infrastructure Engineering, The University of Melbourne, Victoria 3010, Australia

Corresponding authors: Agnès Maurel, agnes.maurel@espci.fr; Kim Pham, kim.pham@ensta.fr

(Received 24 April 2025; revised 14 October 2025; accepted 22 October 2025)

We derive effective Boussinesq and Korteweg–de Vries equations governing nonlinear wave propagation over a structured bathymetry using a three-scale homogenization approach. The model captures the anisotropic effects induced by the bathymetry, leading to significant modifications in soliton dynamics. Homogenized parameters, determined from elementary cell problems, reveal strong directional dependencies in wave speed and dispersion. Our results provide new insights into nonlinear wave propagation in structured shallow-water environments, and consequently motivate further fundamental and applied studies in wave hydrodynamics and coastal engineering.

Key words: nonlinear dynamical systems, solitary waves, surface gravity waves

1. Introduction

The seminal model proposed by Boussinesq (1871) is a reduced-order model for wave propagation in a shallow-water regime over a flat bottom, characterized by weak nonlinearity and weak dispersion. Over the years, numerous extensions of this model have been developed to account for increasingly complex physical phenomena; comprehensive reviews are provided in Madsen & Schäffer (1999) and Brocchini (2013). A significant body of work has focused on the development of reduced Boussinesq-type models for

wave propagation over slowly varying seabed bathymetry, where smooth variations occur on a scale comparable to the wavelength (Madsen & Sørensen 1992; Beji & Nadaoka 1996; Agnon, Madsen & Schäffer 1999; Madsen *et al.* 2002, 2006; Klopman, Van Groesen & Dingemans 2010). The limitations of this regime become evident when the characteristic length of seabed variations is comparable to the water depth, such as in the case of a sharp step or a rapidly oscillating microstructure. In such cases, it becomes necessary to account for evanescent fields around obstacles and potential velocity singularities in the presence of irregular geometries or sudden changes in depth, see for instance Tuck (2005).

Due to the complexity of the nonlinear water-wave problem, most of the literature in this field focuses on the linear regime, which has seen a resurgence of interest due to recent developments in metamaterials for water-wave control. These metamaterials often involve rapidly varying bathymetries composed of rigid vertical plates placed on the seabed (Porter & Newman 2014). Such structures have been experimentally applied to achieve wave manipulation and cloaking (Farhat *et al.* 2008; Berraquero *et al.* 2013; Xu *et al.* 2015; Li *et al.* 2018; Hua *et al.* 2022). Note that, while most studies on water-wave metamaterials focus on linear regimes, a few recent works have explored nonlinear effects, albeit in configurations based on local resonators rather than varying bathymetry (Bobinski *et al.* 2015; Monsalve *et al.* 2019; Lorenzo *et al.* 2023).

Homogenization theories provide a robust framework for understanding the macroscopic behaviour of waves over structured bathymetries. For example, Maurel *et al.* (2017) and Marangos & Porter (2021) demonstrated that the homogenized model of a rapidly oscillating bathymetry accurately reproduces the anisotropy of experimentally determined dispersion relations. Moreover, Maurel, Pham & Marigo (2019) extended this approach to finite-sized bathymetries by deriving homogenized transmission conditions.

That said, the application of homogenization techniques in the nonlinear regime has received significantly less attention. The pioneering work of Rosales & Papanicolaou (1983) introduced an effective Korteweg–de Vries (KdV)-type equation for waves propagating over a periodic microstructure in a two-dimensional setting, using two-scale homogenization techniques. However, it took over two decades for this result to be extended to a three-dimensional and bidirectional framework by Craig *et al.* (2005), who derived a homogenized Boussinesq equation for rapidly varying seabeds using Hamiltonian perturbation theory. Note that in this study, the three-dimensional model assumes a scale separation between the two horizontal directions, as it aims to model an effective Kadomtsev–Petviashvili equation. Simultaneously, Nachbin (2003) proposed a theoretical framework based on conformal mapping techniques to derive one-dimensional Boussinesq-type systems with variable coefficients that depend on terrain-following coordinates. This framework was later generalized to two-dimensional propagation by Andrade & Nachbin (2018). Building on these developments, Garnier, Kraenkel & Nachbin (2007) derived a one-dimensional effective Boussinesq equation with explicit expressions for the homogenized coefficients in the case of sinusoidal bathymetry, recovering the results of Rosales & Papanicolaou (1983). We also note the work of Quezada de Luna & Ketcheson (2021) and Ketcheson, Lóczy & Russo (2025), which adopt a two-step asymptotic approach. In these works, the authors start from a reduced Saint-Venant-type equation, where the vertical structure of the flow is incorporated through an effective water depth that depends on the horizontal coordinates. Homogenization is then applied to this reduced equation. This method assumes slowly varying bathymetry and, in the periodic case, that the period is large compared with the water depth. Despite these advances, extending homogenization techniques to fully three-dimensional settings without horizontal scale separation remains an open challenge.

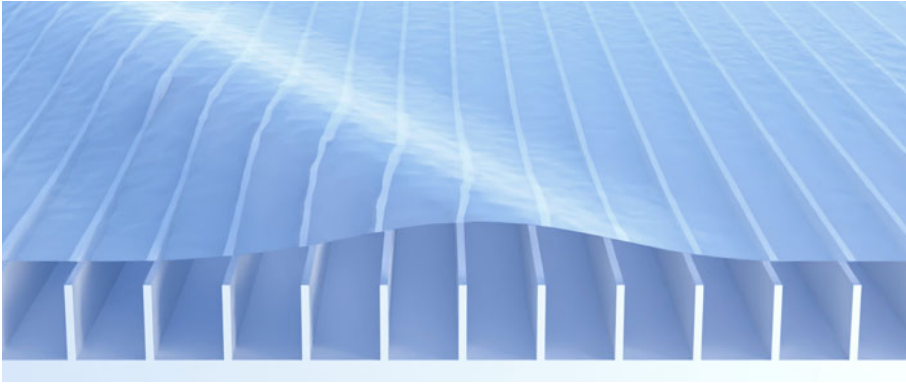


Figure 1. Nonlinear wave propagating obliquely over a structured bathymetry.

In this paper, we revisit the problem considered in Rosales & Papanicolaou (1983) in a three-dimensional setting, focusing on a rapidly oscillating bathymetry that is invariant in one-direction, see figure 1. To this end, we build on the three-scale homogenization framework introduced in Monsalve, Pham & Maurel (2024) for the analysis of step-like topographies in the weakly dispersive and weakly nonlinear regime. This approach involves three scales: the macroscopic scale of the incident wavelength; the mesoscopic scale associated with the varying bathymetry (the so-called periodic elementary cell); the microscopic scale corresponding to the water surface elevation. These scales are connected through asymptotic matching conditions. A key feature of the method is the interpretation of the surface elevation as a boundary layer phenomenon at the mesoscopic scale as well as the accountability of the singularity of the velocity near sharp edges of the bathymetry. We apply this methodology to the case of a periodic bathymetry, recovering the two-dimensional results of Rosales & Papanicolaou (1983). By generalizing the model to three dimensions, without assuming horizontal scale separation, we provide an explicit prediction of the anisotropic effects induced by irregular seabeds on the propagation of KdV solitons.

This article is organized as follows. Section 2 recalls the classical Boussinesq model over a flat bottom and the stationary soliton-type solution of the associated KdV equation. We then introduce the homogenized version of the Boussinesq model for rapidly oscillating bathymetry, involving effective parameters deduced from elementary problems on a unit cell. Due to the anisotropy of the effective medium, the homogenized model leads to an effective KdV equation that depends on the propagation direction of the soliton. Section 2 is devoted to the construction of the homogenized model using a three-scale asymptotic analysis. Finally, in § 3, we analyse the physical properties of the model, with a focus on soliton sensitivity to bathymetric features such as spacing, obstacle height and incidence angle.

2. Anisotropic Boussinesq and KdV models for structured bathymetry

We consider nonlinear propagation of water waves over a structured bathymetry characterized by a periodic alternation of depths between h and ξh , $0 \leq \xi < 1$ and periodicity p relative to the water depth, see figure 2. Assuming an inviscid, incompressible fluid in irrotational motion, the velocity \mathbf{u} and the associated velocity potential φ satisfy

$$\operatorname{div}^{3d} \mathbf{u}(\mathbf{r}, z, t) = 0, \quad \mathbf{u}(\mathbf{r}, z, t) = \nabla^{3d} \varphi(\mathbf{r}, z, t), \quad (2.1)$$

where g is the gravitational constant, t is time, $\mathbf{r} = (x, y)$ represents the coordinate in the horizontal plane and z the vertical coordinate. These equations (2.1) are complemented

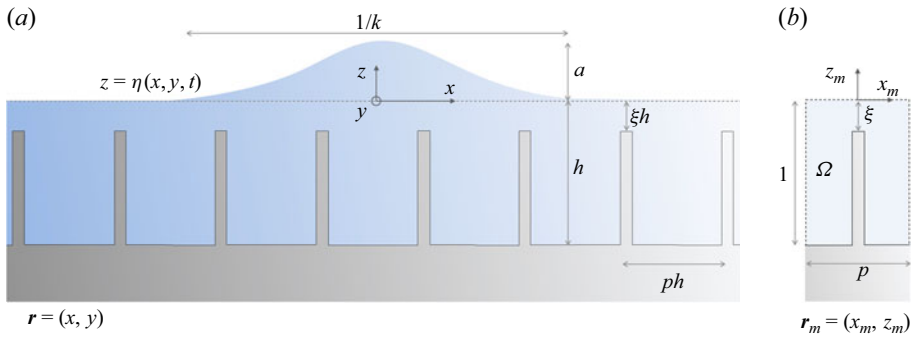


Figure 2. (a) Nonlinear wave propagation over a bathymetry that is periodic in x and invariant in y . (b) The effective wave parameters are derived from elementary problems set in the two-dimensional unit cell Ω using rescaled coordinates $x_m = x/h$ and $z_m = z/h$, and we set $S = |\Omega|$ the unit cell area.

by the nonlinear dynamic and kinematic boundary conditions at the free surface, i.e.

$$\frac{\partial \varphi}{\partial t} + \frac{\mathbf{u} \cdot \mathbf{u}}{2} + g\eta = 0, \quad u_z = \frac{\partial \eta}{\partial t} + \mathbf{u} \cdot \nabla \eta \quad \text{at } z = \eta(\mathbf{r}, t), \quad (2.2)$$

(we have defined $\nabla f = \partial_x f \mathbf{e}_x + \partial_y f \mathbf{e}_y$ and $\nabla^{\text{3d}} f = \nabla f + \partial_z f \mathbf{e}_z$) and condition of vanishing normal velocity

$$\mathbf{u} \cdot \mathbf{n} = 0 \quad \text{on the rigid walls.} \quad (2.3)$$

In the remainder of this section, we first recall the forms of the classical Boussinesq and KdV equations for constant bathymetry. We then present the main contribution of this work, which is the generalization of these equations to the case of a rapidly varying periodic bathymetry.

2.1. The classical Boussinesq and KdV models for a flat bathymetry

For weakly nonlinear and fairly long waves compared with a constant reference water depth h , the classical Boussinesq equations are deduced from the dimensional reduction in the vertical coordinate of (2.1)–(2.3). The resulting, effective, system governing the free surface elevation $\eta(\mathbf{r}, t)$ and the horizontal velocity $\mathbf{u}(\mathbf{r}, t) = u_x(\mathbf{r}, t)\mathbf{e}_x + u_y(\mathbf{r}, t)\mathbf{e}_y$ at the free surface under such hypothesis reads as

$$\begin{cases} \frac{\partial \eta}{\partial t} + \text{div} [(h + \eta)\mathbf{u}] + \frac{h^3}{3} \text{div} [\Delta \mathbf{u}] = 0, \\ \frac{\partial \mathbf{u}}{\partial t} + g \nabla \eta + \frac{1}{2} \nabla (\mathbf{u} \cdot \mathbf{u}) = 0. \end{cases} \quad (2.4)$$

From the Boussinesq equations, a KdV equation can be obtained (see (3.102) and (3.107) in Whitham (2011)) by considering solitary wave solutions of the form $\eta(\mathbf{r}, t) = \eta_0 f(x - ut)$, corresponding to one-directional wave of amplitude η_0 propagating in the \mathbf{e}_x direction with celerity c , leading to

$$\frac{\partial \eta}{\partial t} + c \left(1 + \frac{3}{2} \frac{\eta}{h} \right) \frac{\partial \eta}{\partial x} + \frac{ch^2}{6} \frac{\partial^3 \eta}{\partial x^3} = 0, \quad c = \sqrt{gh}, \quad (2.5)$$

resulting in the form of a soliton of speed u

$$\eta(x, t) = \eta_0 \operatorname{sech}^2 \left\{ \left(\frac{3\eta_0}{4h^3} \right)^{1/2} (x - ut) \right\}, \quad u = c \left(1 + \frac{\eta_0}{2h} \right). \quad (2.6)$$

As expected for a constant depth, the classical Boussinesq and KdV models are isotropic and thus insensitive to the direction of wave propagation.

2.2. Effective model for a periodic bathymetry

In the case of a fast-varying periodic bathymetry, see [figure 2](#), the dimensional reduction of the governing equations leads to an anisotropic version of the Boussinesq and KdV equations previously given by (2.4) and (2.5) in the case of a constant bathymetry. The effective problem is set on the surface elevation $\bar{\eta}(\mathbf{r}, t)$ and velocity $\bar{\mathbf{u}}(\mathbf{r}, t)$ at the free surface, corresponding to averaged versions of the actual field over a periodic cell (hence homogenizing fast oscillations associated with the presence of the periodic microstructure at the bottom).

2.2.1. Anisotropic Boussinesq model

The main result of this study is the derivation of the effective Boussinesq equations for a structured bathymetry, which read as

$$\left\{ \begin{aligned} \frac{\partial \bar{\eta}}{\partial t} + \operatorname{div} [(\alpha_x \bar{h} + n_x \bar{\eta}) \bar{u}_x \mathbf{e}_x + (\bar{h} + \bar{\eta}) \bar{u}_y \mathbf{e}_y] \\ + \bar{h} h^2 \operatorname{div} \left[\left(d_{xx} \frac{\partial^2 \bar{u}_x}{\partial x^2} + d_{xy} \frac{\partial^2 \bar{u}_x}{\partial y^2} \right) \mathbf{e}_x + \left(d_{yx} \frac{\partial^2 \bar{u}_y}{\partial x^2} + d_{yy} \frac{\partial^2 \bar{u}_y}{\partial y^2} \right) \mathbf{e}_y \right] = 0, \\ \frac{\partial \bar{\mathbf{u}}}{\partial t} + g \nabla \bar{\eta} + \frac{1}{2} \nabla (n_x \bar{u}_x^2 + \bar{u}_y^2) = 0, \end{aligned} \right. \quad (2.7)$$

involving the largest depth h and average water depth \bar{h} , a non-dimensional parameter α_x responsible of the anisotropy in the linear non-dispersive regime, four non-dimensional parameters ($d_{xx}, d_{xy}, d_{yx}, d_{yy}$) accounting for the dispersive effects and one non-dimensional parameter n_x encapsulating the effect of the anisotropic microstructure in the nonlinear regime. These parameters are given by the resolution of linear static problems, of the Poisson-type, which depend only on the geometry of the periodic unit cell, see § 2.2.3. For the case of a flat bathymetry, see [tables 1](#) and [2](#), these coefficients become explicit and we recover the classical Boussinesq equations given in (2.4). It should be noted that the Boussinesq system in (2.7) corresponds, in the flat-bed limit of our model, to the so-called Kaup system or the integrable version of the Boussinesq system due to Krishnan (1982). This system has been studied in Chen (1998) and Bona, Chen & Saut (2002) as one of the possible forms, obtained via the Boussinesq trick and modulo a choice of the effective velocity reference level (resulting in a family of so-called a–b–c–d systems). For our model, applying the Boussinesq trick poses no particular difficulty. However, in the presence of a variable bathymetry, the choice of the effective velocity level becomes more delicate and requires revisiting the asymptotic derivation. In particular, it would be necessary to perform the asymptotic analysis for different reference levels to establish the equivalent of the anisotropic a–b–c–d systems and then carry out a corresponding stability study. For now, we highlight this as an important direction for future work.

2.2.2. Anisotropic KdV equation and soliton propagation

A key feature of the effective Boussinesq equations (2.7) is their ability to admit anisotropic soliton-type solutions in the homogenized sense, when the influence of the microstructured bathymetry has been spatially averaged. Considering a one-directional effective solution of the form $\bar{\eta}(\mathbf{r}, t) = \eta_0 f(s - u_\theta t)$, representing a wave of amplitude η_0 propagating along the direction \mathbf{e}_θ , which makes an angle θ with \mathbf{e}_x with celerity u_θ . With $s = \mathbf{r} \cdot \mathbf{e}_\theta$ the local coordinate along the propagation direction, we find the following effective KdV equation:

$$\frac{\partial \bar{\eta}}{\partial t} + c_\theta \left(1 + \frac{3}{2} \frac{\bar{\eta}}{h_\theta} \right) \frac{\partial \bar{\eta}}{\partial s} + \gamma_\theta \frac{c_\theta h_\theta^2}{6} \frac{\partial^3 \bar{\eta}}{\partial s^3} = 0, \quad c_\theta = \sqrt{g H_\theta}, \quad (2.8)$$

where the anisotropic coefficients ($h_\theta, H_\theta, \gamma_\theta$) are defined as

$$\begin{cases} h_\theta = \frac{\alpha_x \cos^2 \theta + \sin^2 \theta}{n_x \cos^2 \theta + \sin^2 \theta} \bar{h}, & H_\theta = (\alpha_x \cos^2 \theta + \sin^2 \theta) \bar{h}, \\ \gamma_\theta = 3 \frac{\bar{h}}{H_\theta} \left(\frac{h}{h_\theta} \right)^2 (d_{xx} \cos^4 \theta + (d_{xy} + d_{yx}) \cos^2 \theta \sin^2 \theta + d_{yy} \sin^4 \theta), \end{cases} \quad (2.9)$$

which yields a θ -dependent soliton given by

$$\bar{\eta}(s, t) = \eta_0 \operatorname{sech}^2 \left\{ \left(\frac{3\eta_0}{4\gamma_\theta h_\theta^3} \right)^{1/2} (s - u_\theta t) \right\}, \quad u_\theta = c_\theta \left(1 + \frac{\eta_0}{2h_\theta} \right). \quad (2.10)$$

A detailed analysis of the property of this θ -dependent soliton is provided in § 4. Note that in the case of a flat bathymetry (see table 2), one recovers $c_\theta = c$, $h_\theta = h$ and $\gamma_\theta = 1$, thus retrieving the classical KdV (2.5) and the isotropic soliton solution (2.6). In the following, we consider the solution (2.10). We emphasize, however, that the stability of the standard KdV equation has been demonstrated by Benjamin (1972) and Bona (1975). With a proper renormalization of (2.8), these stability results directly apply to our anisotropic KdV equation, independently of the propagation direction defined by θ .

2.2.3. Effective parameters and elementary problems

The non-dimensional parameters α_x, n_x and d_{ab} , $\{a, b\} \in \{x, y\}$, governing the Boussinesq (2.7), are computed by solving a sequence of linear, static, Poisson-type problems defined over the periodic unit cell Ω with local coordinates $\mathbf{r}_m = (x_m, z_m) = (x, z)/h$. There are five such elementary problems, denoted $(Q^{(0)}, Q_x^{(1)}, Q_y^{(1)}, Q_x^{(2)}, Q_y^{(2)})$, each satisfying a generic form

$$\begin{cases} \operatorname{div}_m (\nabla_m Q + F \mathbf{e}_x) = G, & \text{in } \Omega, \\ (\nabla_m Q + F \mathbf{e}_x) \cdot \mathbf{n} = 0, & \text{on the walls,} \\ \frac{\partial Q}{\partial z_m}(x_m, 0) = H, \quad \int_{z_m=0} Q(x_m, 0) dx_m = 0, \\ Q, (\nabla_m Q + F \mathbf{e}_x) \text{ } p\text{-periodic with respect to } x_m. \end{cases} \quad (2.11)$$

The source terms $F(\mathbf{r}_m)$, $G(\mathbf{r}_m)$ and $H(x_m)$ vary across the five problems and are given in table 1. Since some elementary problems rely on the solutions of others, they must be

Q :	$Q^{(0)}$	$Q_x^{(1)}$	$Q_y^{(1)}$	$Q_x^{(2)}$	$Q_y^{(2)}$
F :	1	$Q^{(0)}$	0	$Q_x^{(1)}$	$Q_y^{(1)}$
G :	0	$-1 - \frac{\partial Q^{(0)}}{\partial x_m}$	-1	$-Q^{(0)} - \frac{\partial Q_x^{(1)}}{\partial x_m}$	$-Q^{(0)} - \frac{\partial Q_y^{(1)}}{\partial x_m}$
H :	0	$-\frac{\alpha_x S}{p}$	$-\frac{S}{p}$	$-\frac{\alpha_x S}{p} Q^{(0)} _{z_m=0}$	$-\frac{S}{p} Q^{(0)} _{z_m=0}$

Table 1. The five elementary problems follow the same Poisson-type cell problem (2.11). For each, we provide the corresponding bulk sources $F(\mathbf{r}_m)$, $G(\mathbf{r}_m)$ and surface source $H(x_m)$.

Elementary solutions	Effective parameters
$Q^{(0)}(\mathbf{r}_m) = 0$	$\alpha_x = n_x = 1$
$Q_x^{(1)}(\mathbf{r}_m) = Q_y^{(1)}(\mathbf{r}_m) = -\frac{z_m^2}{2} - z_m$	$d_{yx} = d_{yy} = 1/3$
$Q_x^{(2)}(\mathbf{r}_m) = Q_y^{(2)}(\mathbf{r}_m) = 0$	$d_{xx} = d_{xy} = 1/3$

Table 2. Explicit solutions for the elementary problems in the flat bathymetry case (with $S = p$ and $\bar{h} = h$), and the corresponding effective parameters from (2.12)–(2.13).

solved in a sequential order, starting with $Q^{(0)}$, then computing $Q_x^{(1)}$ and $Q_y^{(1)}$, and finally $Q_x^{(2)}$ and $Q_y^{(2)}$.

The effective, dimensionless, parameters α_x and n_x are given by

$$\alpha_x = 1 + \frac{1}{S} \int_{\Omega} \frac{\partial Q^{(0)}}{\partial x_m}(\mathbf{r}_m) d\mathbf{r}_m, \quad n_x = 1 + \frac{1}{p} \int_{z_m=0} \left(\frac{\partial Q^{(0)}}{\partial x_m}(x_m, 0) \right)^2 dx_m, \quad (2.12)$$

where S denotes the area of the unit cell Ω , while the parameters (d_{xx} , d_{xy} , d_{yx} , d_{yy}) are defined by

$$\begin{cases} d_{yx} = \frac{1}{S} \int_{\Omega} Q_x^{(1)}(\mathbf{r}_m) d\mathbf{r}_m, & d_{yy} = \frac{1}{S} \int_{\Omega} Q_y^{(1)}(\mathbf{r}_m) d\mathbf{r}_m, \\ d_{xx} = d_{yx} + \frac{1}{S} \int_{\Omega} \frac{\partial Q_x^{(2)}}{\partial x_m} d\mathbf{r}_m, & d_{xy} = d_{yy} + \frac{1}{S} \int_{\Omega} \frac{\partial Q_y^{(2)}}{\partial x_m} d\mathbf{r}_m. \end{cases} \quad (2.13)$$

For a flat bathymetry, the elementary problems admit explicit solutions, leading to classical values for the effective parameters of the standard Boussinesq model (2.4), as summarized in table 2.

3. Asymptotic derivation of the homogenized Boussinesq model

3.1. Summary of the asymptotic procedure

To capture in a single asymptotic framework the contributions due to nonlinearities and dispersion, we use classical scalings for characteristic wavelength $1/k$, water depth h

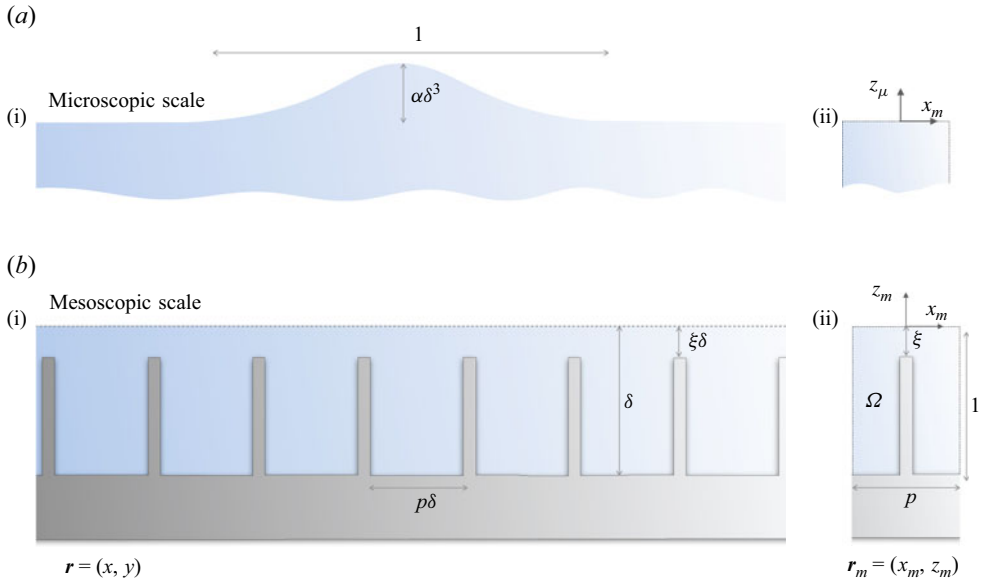


Figure 3. Non-dimensional scales of the problem, from (3.1)–(3.2). (a) The microscopic scale is associated with the wave amplitude $ka = \alpha\delta^3$ (the macroscopic scale is that of the non-dimensional wavelength $O(1)$); (b) the intermediate, mesoscopic, scales are associated with the water depth $kh = \delta$ and array spacing $p\delta = O(\delta)$. Panels (a ii) and (b ii) show the corresponding systems of coordinates in the microscopic domain and in the mesoscopic domain, within the unit cell, see (3.6).

and wave amplitude a . Specifically, by introducing the dimensionless nonlinearity and shallowness parameters

$$\varepsilon = \frac{a}{h} \ll 1, \quad \delta = kh \ll 1. \quad (3.1)$$

Moreover, we consider the following scaling:

$$\varepsilon = \alpha\delta^2, \quad \text{with } \alpha = O(1), \quad (3.2)$$

which ensures a non-trivial interplay between nonlinearities and dispersion as well as keeping a single small parameter δ in the study. In addition, the structured bathymetry has periodicity and step height of the order of h . In the following sections, we will conduct the asymptotic analysis in the different regions shown in figure 3 and, for simplicity, we will consider the non-dimensional form of (2.1)–(2.3). Introducing leading-order dispersion relation $\omega = \sqrt{gh}k$, we use the following transformations:

$$t \rightarrow \omega t, \quad (x, y, z) \rightarrow k(x, y, z), \quad \eta \rightarrow \eta/a, \quad \mathbf{u} \rightarrow \mathbf{u}/(\omega a), \quad \varphi \rightarrow k\varphi/(\omega a), \quad (3.3)$$

which provide the non-dimensional form of (2.1). The incompressibility (Inc), and irrotationality conditions (Rot) become

$$(\text{Inc}) : \operatorname{div}^{3d} \mathbf{u} = 0, \quad (\text{Rot}) : \mathbf{u} = \nabla^{3d} \varphi, \quad (3.4)$$

while the dynamic (DC) and kinematic (KC) conditions at the free surface, described by (2.2) and (2.3), as well as the vanishing normal velocity on the rigid walls formed by the

seabed at and the walls (RC) read

$$\begin{aligned} \text{(DC): } \frac{\partial \varphi}{\partial t} + \varepsilon \delta \frac{\mathbf{u} \cdot \mathbf{u}}{2} + \delta^{-1} \eta &= 0, & \text{(KC): } u_z &= \frac{\partial \eta}{\partial t} + \varepsilon \delta \mathbf{u} \cdot \nabla \eta, & \text{at } z &= \varepsilon \delta \eta(\mathbf{r}, t), \\ \text{(RC): } \mathbf{u} \cdot \mathbf{n} &= 0 & \text{on the walls.} \end{aligned} \quad (3.5)$$

In the above equations, we distinguish three different scales. We first have the macroscopic scale which concerns the horizontal variations that occur at the wavelength scale. Next, we have the mesoscopic scale, which is associated with the scale of the water depth and the bathymetry. Finally, we have the microscopic scale which governs the scale of the wave amplitude $\varepsilon \delta$ in the vicinity of the free surface. Note that the macroscopic and mesoscopic scales are classic for linear shallow-water waves, while the microscale is linked to the (weakly) nonlinear context. This microscopic region corresponds to a zoom revealing the finite wave amplitude, very small compared with the water depth (strictly zero in a linear analysis), and its study will provide the boundary condition for the mesoscopic region. Based on these considerations, we introduce rescaled coordinates capable of taking these different scales into account vertically and horizontally,

$$\text{macro: } \mathbf{r} = (x, y), \quad \text{meso: } \mathbf{r}_m = (x_m, z_m) = \left(\frac{x}{\delta}, \frac{z}{\delta} \right), \quad \text{micro: } z_\mu = \frac{z_m - \varepsilon \eta}{\varepsilon \eta}. \quad (3.6)$$

At the mesoscopic scale in the region of the bathymetry or at the microscopic scale near the free surface, the procedure consists in using the appropriate spatial coordinates (3.6) to get a unitary domain that depends neither on δ or ε (it has $O(1)$ dimensions) while the dependence on the small parameter appears explicitly in a new system of equations. The two regions are then connected by asymptotically matching their solutions.

3.2. Setting of the multiscale problem

3.2.1. The mesoscopic domain

The mesoscopic domain Ω consists of a two-dimensional periodic cell of vertical extend δ and horizontal unitary extend. It includes the microstructural bathymetry at the sea bottom but it excludes the free surface of vertical extend $\varepsilon \delta \ll \delta$, see figure 3. At this scale, the fields follow a two-scale expansion with respect to the macroscopic scale \mathbf{r} and mesoscopic scale \mathbf{r}_m ,

$$\mathbf{u} = \sum_{n \geq 0} \delta^n \mathbf{u}^{(n)}(\mathbf{r}, \mathbf{r}_m, t), \quad \varphi = \sum_{n \geq 0} \delta^n \varphi^{(n)}(\mathbf{r}, \mathbf{r}_m, t), \quad (3.7)$$

with $\mathbf{u}^{(n)}$ and $\varphi^{(n)}$ being p -periodic with respect to x_m . The differential operator is thus redefined as

$$\nabla^{3d} \rightarrow \nabla + \frac{1}{\delta} \nabla_m, \quad \nabla_m = \mathbf{e}_x \frac{\partial}{\partial x_m} + \mathbf{e}_z \frac{\partial}{\partial z_m}, \quad (3.8)$$

and it follows that (3.4)–(3.5) in the mesoscopic domain read

$$\begin{aligned} {}^m(\text{Inc}): \quad \text{div} \mathbf{u} + \frac{1}{\delta} \text{div}_m \mathbf{u} &= 0, & {}^m(\text{Rot}): \quad \mathbf{u} &= \nabla \varphi + \frac{1}{\delta} \nabla_m \varphi, \\ {}^m(\text{RC}): \quad \mathbf{u} \cdot \mathbf{n} &= 0 & \text{on the walls.} \end{aligned} \quad (3.9)$$

We insist on the fact that the mesoscopic region excludes the free surface: the values of the fields at $z_m = 0$ are unknowns at this stage and their determination will result from a matched asymptotic analysis with the microscopic domain introduced in the next section.

3.2.2. The microscopic domain

The microscopic domain is the region located at the free surface which results from a zoom made at a point x_m near the boundary $z_m = 0$ in the mesoscopic domain. It corresponds to a water column of infinite vertical extent where nonlinearities are governed by the dynamic/kinematic boundary conditions at the free surface. Here, we have to account for the variations of the fields on the macroscopic scale over x and y , on the mesoscopic scale over x_m but now over the microscopic scale z_μ . Accordingly, we have a three-scale expansion as follows:

$$\mathbf{u} = \sum_{n \geq 0} \delta^n \mathbf{v}^{(n)}(\mathbf{r}, x_m, z_\mu, t), \quad \varphi = \sum_{n \geq 0} \delta^n \psi^{(n)}(\mathbf{r}, x_m, z_\mu, t), \quad \eta = \sum_{n \geq 1} \delta^n \eta^{(n)}(\mathbf{r}, x_m, t). \quad (3.10)$$

The differential operator reads at this scale

$$\nabla^{3d} \rightarrow \nabla + \frac{\mathbf{e}_x}{\delta} \frac{\partial}{\partial x_m} + \frac{\mathbf{e}_z}{\alpha \delta^3 \eta} \frac{\partial}{\partial z_\mu}. \quad (3.11)$$

It follows that (3.4)–(3.5) in the microscopic domain become

$$\begin{aligned} \mu(\text{Inc}): \quad \text{div} \mathbf{u} + \frac{1}{\delta} \frac{\partial u_x}{\partial x_m} + \frac{1}{\alpha \delta^3 \eta} \frac{\partial u_z}{\partial z_\mu} &= 0, \\ \mu(\text{Rot}): \quad u_x &= \frac{\partial \varphi}{\partial x} + \frac{1}{\delta} \frac{\partial \varphi}{\partial x_m}, \quad u_y = \frac{\partial \varphi}{\partial y}, \quad u_z = \frac{1}{\alpha \delta^3 \eta} \frac{\partial \varphi}{\partial z_\mu}, \end{aligned} \quad (3.12)$$

along with

$$\begin{aligned} \mu(\text{DC}): \quad \frac{\partial \varphi}{\partial t} + \delta^{-1} \eta + \alpha \delta^3 \frac{\mathbf{u} \cdot \mathbf{u}}{2} &= 0, \\ \mu(\text{KC}): \quad u_z &= \frac{\partial \eta}{\partial t} + \alpha \delta^3 \left(\mathbf{u} \cdot \nabla \eta + \frac{1}{\delta} u_x \frac{\partial \eta}{\partial x_m} \right), \quad \text{at } z_\mu = 0. \end{aligned} \quad (3.13)$$

Note that we have anticipated from $\mu(\text{DC})$ and $\mu(\text{KC})$ that $\varphi = O(1)$ implies η and u_z are $O(\delta)$, hence $v_z^{(0)} = \eta^{(0)} = 0$ in (3.10). These equations have to be complemented with appropriate conditions where $z_\mu \rightarrow -\infty$ which correspond to matching conditions with the mesoscopic region as we will see in the next subsubsection.

3.2.3. Matching the solutions in the mesoregions and microregions

The missing conditions that we have identified in the mesodomain and microdomain are provided simultaneously by matching the solutions in an intermediate region when $z_m \rightarrow 0$ and $z_\mu \rightarrow -\infty$, see figure 3. Specifically, for φ , we need to have

$$\varphi^{(0)}(\mathbf{r}, \mathbf{r}_m, t) + \delta \varphi^{(1)}(\mathbf{r}, \mathbf{r}_m, t) + \dots \sim \psi^{(0)}(\mathbf{r}, x_m, z_\mu, t) + \delta \psi^{(1)}(\mathbf{r}, x_m, z_\mu, t) + \dots \quad (3.14)$$

The matching procedure is the same for the other fields. Taking into account (3.6) and using the Taylor expansion

$$f(\mathbf{r}, x_m, z_m, t) = f(\mathbf{r}, x_m, 0, t) + \alpha \delta^2 (z_\mu + 1) \eta(\mathbf{r}, x_m, t) \frac{\partial f}{\partial z_m}(\mathbf{r}, x_m, 0, t) + \dots, \quad (3.15)$$

we identify in (3.14) the terms of the same power of δ , which gives

$$\left\{ \begin{array}{l} \varphi^{(n)}(\mathbf{r}, x_m, 0, t) = \lim_{z_\mu \rightarrow -\infty} \psi^{(n)}(\mathbf{r}, x_m, z_\mu, t), \quad n = 0, 1, 2, \\ \varphi^{(3)}(\mathbf{r}, x_m, 0, t) = \lim_{z_\mu \rightarrow -\infty} \left(\psi^{(3)}(\mathbf{r}, x_m, z_\mu, t) \right. \\ \left. - \alpha(z_\mu + 1)\eta^{(1)}(\mathbf{r}, x_m, t) \frac{\partial \varphi^{(0)}}{\partial z_m}(\mathbf{r}, x_m, 0, t) \right). \end{array} \right. \quad (3.16)$$

The same relations are obtained by replacing $\varphi^{(n)}$ by $u_x^{(n)}$ or $u_z^{(n)}$ and $\psi^{(n)}$ by $v_x^{(n)}$ or $v_z^{(n)}$.

3.2.4. The macroscopic fields

We aim at obtaining equations on macroscopic fields which depend only on \mathbf{r} and t . The fields are defined by averaging the following fields at the free surface X_m :

$$\begin{aligned} \bar{\varphi}^{(n)}(\mathbf{r}, t) &= \frac{1}{p} \int_{X_m} \varphi^{(n)}(\mathbf{r}, x_m, 0, t) dx_m, \quad \bar{\mathbf{u}}^{(n+1)}(\mathbf{r}, t) = \nabla \bar{\varphi}^{(n)}(\mathbf{r}, t), \\ \bar{\eta}^{(n)}(\mathbf{r}, t) &= \frac{1}{p} \int_{X_m} \eta^{(n)}(\mathbf{r}, x_m, t) dx_m, \end{aligned} \quad (3.17)$$

and as an intermediate mean field we shall also use the average horizontal velocity in the unit cell

$$\mathbf{U}^{(n)}(\mathbf{r}, t) = \frac{1}{S} \int_{\Omega} \left(u_x^{(n)}(\mathbf{r}, \mathbf{r}_m, t) \mathbf{e}_x + u_y^{(n)}(\mathbf{r}, \mathbf{r}_m, t) \mathbf{e}_y \right) d\mathbf{r}_m. \quad (3.18)$$

3.3. Resolution at orders zero and one: non-dispersive linear behaviour

PROPOSITION 3.1. *The effective wave equation reads at the dominant orders $n = 0, 1$,*

$$\left\{ \begin{array}{l} \frac{\partial \bar{\varphi}^{(n)}}{\partial t} + \bar{\eta}^{(n+1)} = 0, \quad \operatorname{div} \mathbf{U}^{(n)} + \kappa \frac{\partial \bar{\eta}^{(n+1)}}{\partial t} = 0, \end{array} \right. \quad (3.19a)$$

$$\left\{ \begin{array}{l} \mathbf{U}^{(n)} = \alpha_x \frac{\partial \bar{\varphi}^{(n)}}{\partial x} \mathbf{e}_x + \frac{\partial \bar{\varphi}^{(n)}}{\partial y} \mathbf{e}_y, \end{array} \right. \quad (3.19b)$$

with $\kappa = (p/S)$ and α_x given by (2.12).

Remark. At these dominant orders, the effect of the microstructure is already visible since the wave equation is anisotropic, however, the effects of dispersion and nonlinearities are not captured. In the absence of microstructure, i.e. a flat bathymetry, see table 2, we simply obtain the linear isotropic wave equation in shallow water.

3.3.1. Proof of (3.19) for $n = 0$

From ${}^m(\operatorname{Rot})^{-1}$ in (3.9), we have $\nabla_m \varphi^{(0)} = 0$, and from ${}^\mu(\operatorname{Rot})_x^{-1}$ and ${}^\mu(\operatorname{Rot})_z^{-4}$ in (3.12), $\partial_{x_m} \psi^{(0)} = \partial_{z_\mu} \psi^{(0)} = 0$, hence $\psi^{(0)} = \psi^{(0)}(\mathbf{r}, t)$. Owing to the matching (3.16), we deduce

$$\psi^{(0)}(\mathbf{r}, t) = \varphi^{(0)}(\mathbf{r}, t). \quad (3.20)$$

Next, from ${}^{\mu}(\text{Inc})^{-3}$ in (3.12), $\partial_{z_{\mu}} v_z^{(1)} = 0$. Accounting for ${}^{\mu}(\text{KC})^1$ and ${}^{\mu}(\text{DC})^0$ as well as the matching on $u_z^{(1)}$ from (3.16), we obtain

$$v_z^{(1)}(\mathbf{r}, t) = -\frac{\partial^2 \psi^{(0)}}{\partial t^2}(\mathbf{r}, t) = \frac{\partial \eta^{(1)}}{\partial t}(\mathbf{r}, t) = u_z^{(1)}(\mathbf{r}, x_m, z_m = 0, t), \quad (3.21)$$

which tells us that $u_z^{(1)}$ does not depend on x_m . By integrating (3.21) over X_m together with (3.20), we obtain the first relation in (3.19a) for $n = 0$. Now, we use ${}^m(\text{Inc})^0$ in (3.9), namely $\text{div}_m \mathbf{u}^{(0)} + \text{div}_m \mathbf{u}^{(1)} = 0$, that we integrate over Ω . By doing so and accounting for the boundary condition ${}^m(\text{RC})^1$ in (3.9) on the walls and for the p -periodicity of $\mathbf{u}^{(1)}$ with respect to x_m , we obtain

$$\mathbf{S} \text{div} \mathbf{U}^{(0)} + \int_{X_m} u_z^{(1)}(\mathbf{r}, x_m, z_m = 0, t) \, dx_m = 0, \quad (3.22)$$

where the second term is deduced from (3.21) and we obtain the second relation in (3.19a) for $n = 0$.

The relation (3.19b) is obtained by considering the problem satisfied by $(\mathbf{u}^{(0)}, \varphi^{(1)})$ in the $\mathbf{r}_m \in \Omega$ coordinate. From ${}^m(\text{Inc})^{-1}$, ${}^m(\text{Rot})^0$, ${}^m(\text{RC})^0$ in (3.9) along with the matching condition (3.16) which provides $u_z^{(0)}(\mathbf{r}, x_m, z_m = 0) = 0$ (since $v_z^{(0)} = 0$), the problem reads

$$\begin{cases} \text{div}_m \mathbf{u}^{(0)} = 0, & \mathbf{u}^{(0)} = \nabla_m \varphi^{(1)} + \nabla \bar{\varphi}^{(0)}(\mathbf{r}, t), & \text{in } \Omega, \\ \mathbf{u}^{(0)} \cdot \mathbf{n} = 0 \text{ on the walls, } & u_z^{(0)} = 0 \text{ at } z_m = 0, \\ \mathbf{u}^{(0)}, \varphi^{(1)} & p\text{-periodic with respect to } x_m. \end{cases} \quad (3.23)$$

The above problem is linear with respect to the two components of $\nabla \bar{\varphi}^{(0)}$ and noticing that $\mathbf{r}_m \cdot \mathbf{e}_y = 0$, the solution can be written as

$$\varphi^{(1)} = \bar{\varphi}^{(1)} + \frac{\partial \bar{\varphi}^{(0)}}{\partial x} Q^{(0)}, \quad (3.24)$$

with $\bar{\varphi}^{(1)}$ defined in (3.17) and $Q^{(0)}(\mathbf{r}_m)$ solution to the elementary problem announced in (2.11) and table 1.

Integrating $\mathbf{u}^{(0)} = \nabla_m \varphi^{(1)} + \nabla \bar{\varphi}^{(0)}$ (with (3.24)) over Ω , see (3.17), we obtain (3.19b) with α_x given by (2.12).

3.3.2. Proof of (3.19) for $n = 1$

We proceed as for $n = 0$. From ${}^{\mu}(\text{Rot})_z^{-3}$ in (3.12), $\partial_{z_{\mu}} \psi^{(1)} = 0$, and from ${}^{\mu}(\text{Rot})_{x,y}^0$ in (3.12), ${}^m(\text{Rot})_{x,y}^0$ in (3.9) and (3.20) (along with the matchings (3.16)), we have

$$\psi^{(1)}(\mathbf{r}, x_m, t) = \varphi^{(1)}(\mathbf{r}, x_m, 0, t), \quad v_a^{(0)}(\mathbf{r}, x_m, t) = u_a^{(0)}(\mathbf{r}, x_m, 0, t), \quad a = x, y. \quad (3.25)$$

Next, from ${}^{\mu}(\text{Inc})^{-2}$ in (3.12), $\partial_{z_{\mu}} v_z^{(2)} = 0$ hence from ${}^{\mu}(\text{KC})^2$ and ${}^{\mu}(\text{DC})^1$, along with the matching $u_z^{(2)}$ in (3.16), we obtain

$$v_z^{(2)}(\mathbf{r}, x_m, t) = -\frac{\partial^2 \varphi^{(1)}}{\partial t^2}(\mathbf{r}, x_m, 0, t) = \frac{\partial \eta^{(2)}}{\partial t}(\mathbf{r}, x_m, t) = u_z^{(2)}(\mathbf{r}, x_m, 0, t), \quad (3.26)$$

whose integration over X_m provides the first relation in (3.19a) for $n = 1$. Now, we use ${}^m(\text{Inc})^1$ in (3.9), namely $\text{div}_m \mathbf{u}^{(1)} + \text{div}_m \mathbf{u}^{(2)} = 0$, that we integrate over Ω . Proceeding as previously, we obtain

$$S \text{div} \mathbf{U}^{(1)} + \int_{X_m} u_z^{(2)}(\mathbf{r}, x_m, 0, t) \, dx_m = 0, \quad (3.27)$$

and using (3.26), we obtain the second relation in (3.19a) for $n = 1$.

We now consider the problem satisfied by $(\mathbf{u}^{(1)}, \varphi^{(2)})$ in $\mathbf{r}_m \in \Omega$ coordinate. From ${}^m(\text{Inc})^0$, ${}^m(\text{Rot})^1$, ${}^m(\text{RC})^1$ in (3.9) and (3.21), the problem reads

$$\left\{ \begin{array}{l} \text{div}_m \mathbf{u}^{(1)} = -\text{div} \mathbf{u}^{(0)}, \quad \mathbf{u}^{(1)} = \nabla_m \varphi^{(2)} + \nabla \varphi^{(1)}, \quad \text{in } \Omega, \\ \mathbf{u}^{(1)} \cdot \mathbf{n} = 0 \text{ on the walls,} \quad u_z^{(1)} = -\frac{\partial^2 \bar{\varphi}^{(0)}}{\partial t^2} \text{ at } z_m = 0, \\ \mathbf{u}^{(1)}, \varphi^{(2)} p\text{-periodic with respect to } x_m. \end{array} \right. \quad (3.28)$$

We know $(\mathbf{u}^{(0)}, \varphi^{(1)})$ from (3.24) and we use that $\partial_{tt} \bar{\varphi}^{(0)} = 1/\kappa (\alpha_x \partial_{xx} \bar{\varphi}^{(0)} + \partial_{yy} \bar{\varphi}^{(0)})$ from (3.19a)–(3.19b). The solution at this order can be express as a linear combination of elementary solutions pondered by macroscopic sources. Accordingly, we set

$$\varphi^{(2)} = \bar{\varphi}^{(2)} + \frac{\partial \bar{\varphi}^{(1)}}{\partial x} Q^{(0)} + \frac{\partial^2 \bar{\varphi}^{(0)}}{\partial x^2} Q_x^{(1)} + \frac{\partial^2 \bar{\varphi}^{(0)}}{\partial y^2} Q_y^{(1)}, \quad (3.29)$$

(and $\mathbf{u}^{(1)}$ given in Appendix A.1) with $\bar{\varphi}^{(2)}$ defined in (3.17), $Q^{(0)}(\mathbf{r}_m)$, $Q_x^{(1)}(\mathbf{r}_m)$ and $Q_y^{(1)}(\mathbf{r}_m)$ solutions to the elementary problems given in (2.11) and table 1.

We notice that $Q_x^{(1)}$ and $Q_y^{(1)}$ are even functions of x_m (with $Q^{(0)}$ an odd function of x_m) due to the symmetry $x_m \mapsto -x_m$ of the obstacle. Accordingly, integrating $\mathbf{u}^{(1)} = \nabla_m \varphi^{(2)} + \nabla \varphi^{(1)}$ over Ω (with (3.24) and (3.29), see also Appendix A.1 for the explicit expression of $\mathbf{u}^{(1)}$), we obtain (3.19b) at order $n = 1$.

3.4. Resolution at order two: dispersive contributions

PROPOSITION 3.2. *The effective wave equation reads at the order $n = 2$,*

$$\left\{ \begin{array}{l} \frac{\partial \bar{\varphi}^{(2)}}{\partial t} + \bar{\eta}^{(3)} = 0, \quad \text{div} \mathbf{U}^{(2)} + \kappa \frac{\partial \bar{\eta}^{(3)}}{\partial t} = 0, \end{array} \right. \quad (3.30a)$$

$$\left\{ \begin{array}{l} U_x^{(2)} = \alpha_x \frac{\partial \bar{\varphi}^{(2)}}{\partial x} + d_{xx} \frac{\partial^3 \bar{\varphi}^{(0)}}{\partial x^3} + d_{xy} \frac{\partial^3 \bar{\varphi}^{(0)}}{\partial x \partial y^2}, \end{array} \right. \quad (3.30b)$$

$$\left\{ \begin{array}{l} U_y^{(2)} = \frac{\partial \bar{\varphi}^{(2)}}{\partial y} + d_{yx} \frac{\partial^3 \bar{\varphi}^{(0)}}{\partial x^2 \partial y} + d_{yy} \frac{\partial^3 \bar{\varphi}^{(0)}}{\partial y^3}, \end{array} \right. \quad (3.30c)$$

where $(d_{xx}, d_{xy}, d_{yx}, d_{yy})$ are defined in (2.13).

Remark. Anisotropic dispersive terms appear at this order while nonlinear contributions remains absent. In the absence of microstructure, i.e. a flat bathymetry, see table 2, all the dispersive coefficients d_{ij} are equal to 1/3.

3.4.1. Proof of (3.30)

We start with the equivalent at order two of relations (3.25) and (3.26). First, from ${}^\mu(\text{Rot})_z^{-2}$ in (3.12), we have $\partial_{z\mu}\psi^{(2)} = 0$, and from ${}^\mu(\text{Rot})_{x,y}^1$ in (3.12), ${}^m(\text{Rot})_{x,y}^1$ in (3.9) and (3.25) (along with the matchings (3.16)), we have

$$\psi^{(2)}(\mathbf{r}, x_m, t) = \varphi^{(2)}(\mathbf{r}, x_m, 0, t), \quad v_a^{(1)}(\mathbf{r}, x_m, t) = u_a^{(1)}(\mathbf{r}, x_m, 0, t), \quad a = x, y. \quad (3.31)$$

Next, from ${}^\mu(\text{Inc})^{-1}$ in (3.12) and (3.25), we have $\partial_{z\mu}v_z^{(3)} = -\alpha\eta^{(1)}\partial_{x_m}u_x^{(0)}|_{z_m=0}$. We obtain $v_z^{(3)}$ by integration and using that $v_z^{(3)} = \partial_t\eta^{(3)}$ at $z_\mu = 0$ from ${}^\mu(\text{KC})^3$ in (3.13) along with (3.21). With $\eta^{(3)}$ satisfying ${}^\mu(\text{DC})^2$, we eventually obtain

$$\begin{aligned} v_z^{(3)}(\mathbf{r}, x_m, z_\mu, t) &= \frac{\partial\eta^{(3)}}{\partial t}(\mathbf{r}, x_m, t) - z_\mu\alpha\frac{\partial}{\partial x_m}(\eta^{(1)}(\mathbf{r}, t)u_x^{(0)}(\mathbf{r}, x_m, 0, t)), \\ \eta^{(3)}(\mathbf{r}, x_m, t) + \frac{\partial\varphi^{(2)}}{\partial t}(\mathbf{r}, x_m, 0, t) &= 0, \end{aligned} \quad (3.32)$$

and taking the average over X_m of the second relation above provides the first relation in (3.30a). Using further the matching (3.16) on $u_z^{(3)}$, we also obtain

$$u_z^{(3)}(\mathbf{r}, x_m, 0, t) = \frac{\partial\eta^{(3)}}{\partial t}(\mathbf{r}, x_m, t) + \alpha\frac{\partial}{\partial x_m}(\eta^{(1)}(\mathbf{r}, t)u_x^{(0)}(\mathbf{r}, x_m, 0, t)). \quad (3.33)$$

Now, we use ${}^m(\text{Inc})^2$ in (3.9), namely $\text{div}\mathbf{u}^{(2)} + \text{div}_m\mathbf{u}^{(3)} = 0$, that we integrate over Ω . By doing so and accounting for the boundary condition ${}^m(\text{RC})^3$ in (3.9), we obtain

$$S\text{div}\mathbf{U}^{(2)} + \int_{X_m} u_z^{(3)}(\mathbf{r}, x_m, 0, t) \, dx_m = 0. \quad (3.34)$$

Reporting (3.33) in the last integral and using the p -periodicity of $\eta^{(1)}u_x^{(0)}$ with respect to x_m , we obtain the second relation in (3.30a).

We consider the problem satisfied by $(\mathbf{u}^{(2)}, \varphi^{(3)})$ in $\mathbf{r}_m \in \Omega$ coordinate. From ${}^m(\text{Inc})^1$, ${}^m(\text{Rot})^2$, ${}^m(\text{RC})^2$ in (3.9) and with $u_z^{(2)}$ at $z_m = 0$ given by (3.26), the problem reads

$$\begin{cases} \text{div}_m\mathbf{u}^{(2)} = -\text{div}\mathbf{u}^{(1)}, & \mathbf{u}^{(2)} = \nabla_m\varphi^{(3)} + \nabla\varphi^{(2)}, & \text{in } \Omega, \\ \mathbf{u}^{(2)} \cdot \mathbf{n} = 0 \text{ on the walls,} & u_z^{(2)} = -\frac{\partial^2\varphi^{(1)}}{\partial t^2} \text{ at } z_m = 0, \\ \mathbf{u}^{(2)}, \varphi^{(3)} & p\text{-periodic with respect to } x_m. \end{cases} \quad (3.35)$$

We know $(\mathbf{u}^{(1)}, \varphi^{(2)})$ from (3.28) and (3.29), and $\varphi^{(1)}$ from (3.24), and this tells us that the problem is linear with respect to the two components of $\nabla\bar{\varphi}^{(2)}$, $\partial_{xx}\bar{\varphi}^{(1)}$ and $\partial_{yy}\bar{\varphi}^{(1)}$ (as at order one) as well as $\partial_{xx}\bar{\varphi}^{(0)}$ and $\partial_{xy}\bar{\varphi}^{(0)}$ (see Appendix A.2 for the detailed derivation). Accordingly, we set

$$\varphi^{(3)} = \bar{\varphi}^{(3)} + \frac{\partial\bar{\varphi}^{(2)}}{\partial x}Q^{(0)} + \frac{\partial^2\bar{\varphi}^{(1)}}{\partial x^2}Q_x^{(1)} + \frac{\partial^2\bar{\varphi}^{(1)}}{\partial y^2}Q_y^{(1)} + \frac{\partial^3\bar{\varphi}^{(0)}}{\partial x^3}Q_x^{(2)} + \frac{\partial^3\bar{\varphi}^{(0)}}{\partial x\partial y^2}Q_y^{(2)}, \quad (3.36)$$

with $\mathbf{u}^{(2)}$ (given in Appendix A.1), $\bar{\varphi}^{(3)}$ defined in (3.17) with the two additional functions $Q_x^{(2)}$ and $Q_y^{(2)}$ appearing at this order, solution of the static elementary problems defined in (2.11) and table 1.

We note that $Q_x^{(2)}$ and $Q_y^{(2)}$ are odd functions of x_m (with $Q_{x,y}^{(1)}$ and $Q^{(0)}$ being even and odd functions of x_m , respectively). Accordingly, integrating $\mathbf{u}^{(2)} = \nabla_m \varphi^{(3)} + \nabla \varphi^{(2)}$ in (3.35) over Ω with (3.29) and (3.36) (see also Appendix A.1 for the full expression of $\mathbf{u}^{(2)}$), we obtain the form of $\mathbf{U}^{(2)}$ announced in (3.30b). Eventually, in the absence of microstructure, with $Q^{(0)} = 0$, $Q_x^{(1)}$ and $Q_y^{(1)}$ independent of x_m , we recover that $Q_x^{(2)} = Q_y^{(2)} = 0$, as announced in table 2.

3.5. Resolution at order three: nonlinear contributions

PROPOSITION 3.3. *The effective wave equation reads at order $n = 3$,*

$$\left\{ \begin{array}{l} \frac{\partial \bar{\varphi}^{(3)}}{\partial t} + \bar{\eta}^{(4)} + \frac{\alpha}{2} \left(n_x \left(\frac{\partial \bar{\varphi}^{(0)}}{\partial x} \right)^2 + \left(\frac{\partial \bar{\varphi}^{(0)}}{\partial y} \right)^2 \right) = 0, \\ \operatorname{div} \mathbf{U}^{(3)} + \kappa \left(\frac{\partial \bar{\eta}^{(4)}}{\partial t} + \alpha \operatorname{div}(\bar{\eta}^{(1)} \nabla \bar{\varphi}^{(0)}) \right) = 0, \end{array} \right. \quad (3.37a)$$

$$\left\{ \begin{array}{l} U_x^{(3)} = \alpha_x \frac{\partial \bar{\varphi}^{(3)}}{\partial x} + d_{xx} \frac{\partial^3 \bar{\varphi}^{(1)}}{\partial x^3} + d_{xy} \frac{\partial^3 \bar{\varphi}^{(1)}}{\partial x \partial y^2} - \alpha \kappa (1 - n_x) \frac{\partial \bar{\varphi}^{(0)}}{\partial x} \bar{\eta}^{(1)}, \\ U_y^{(3)} = \frac{\partial \bar{\varphi}^{(3)}}{\partial y} + d_{yx} \frac{\partial^3 \bar{\varphi}^{(1)}}{\partial x^2 \partial y} + d_{yy} \frac{\partial^3 \bar{\varphi}^{(1)}}{\partial y^3}, \end{array} \right. \quad (3.37b)$$

$$\left\{ \begin{array}{l} U_x^{(3)} = \frac{\partial \bar{\varphi}^{(3)}}{\partial x} + d_{xx} \frac{\partial^3 \bar{\varphi}^{(1)}}{\partial x^3} + d_{xy} \frac{\partial^3 \bar{\varphi}^{(1)}}{\partial x \partial y^2} - \alpha \kappa (1 - n_x) \frac{\partial \bar{\varphi}^{(0)}}{\partial x} \bar{\eta}^{(1)}, \\ U_y^{(3)} = \frac{\partial \bar{\varphi}^{(3)}}{\partial y} + d_{yx} \frac{\partial^3 \bar{\varphi}^{(1)}}{\partial x^2 \partial y} + d_{yy} \frac{\partial^3 \bar{\varphi}^{(1)}}{\partial y^3}, \end{array} \right. \quad (3.37c)$$

where n_x and α_x are given by (2.12), and $(d_{xx}, d_{xy}, d_{yx}, d_{yy})$ are defined in (2.13).

Remark. A nonlinear anisotropic contribution appears in (3.37a) at this order. Such contribution becomes isotropic in the absence of microstructure (with $\kappa = n_x = 1$). Note that the nonlinear contribution in (3.37b) vanishes also for $n_x = 1$ in the absence of a microstructure.

3.5.1. Proof of (3.37)

From ${}^\mu(\operatorname{Rot})_z^{-1}$ in (3.12), $\partial_{z_\mu} \psi^{(3)} = 0$, hence from the matching (3.16) along with $\partial_{z_m} \varphi^{(0)} = 0$ from (3.20), we deduce

$$\psi^{(3)}(\mathbf{r}, x_m, t) = \varphi^{(3)}(\mathbf{r}, x_m, 0, t). \quad (3.38)$$

Using the result above along with ${}^\mu(\operatorname{DC})^3$ in (3.13) and (3.25), we have

$$\frac{\partial \varphi^{(3)}}{\partial t}(\mathbf{r}, x_m, 0, t) + \eta^{(4)}(\mathbf{r}, x_m, t) + \frac{\alpha}{2} \left((u_x^{(0)})^2 + (u_y^{(0)})^2 \right)_{|z_m=0} = 0, \quad (3.39)$$

with $(u_x^{(0)}, u_y^{(0)})$ given in (3.23) together with (3.24). Integrating (3.39) over X_m and accounting for the periodicity of $Q^{(0)}$ with respect to x_m provides the first relation in (3.37a).

We now consider $v_z^{(4)}$ which is given by ${}^\mu(\operatorname{Inc})^0$ in (3.12). Using (3.25) and (3.31) along with ${}^m(\operatorname{Inc})^{-1,0}$ in (3.9), we obtain $\partial_{z_\mu} v_z^{(4)} = \alpha \partial_{z_m} (\eta^{(1)} u_z^{(1)} + \eta^{(2)} u_z^{(0)})_{|z_m=0}$. By integration, and using ${}^\mu(\operatorname{KC})^4$ in (3.13) with $\eta^{(1)}$ independent of x_m from (3.21), we obtain

$$\begin{aligned} v_z^{(4)} &= z_\mu \alpha \frac{\partial}{\partial z_m} (\eta^{(1)} u_z^{(1)} + \eta^{(2)} u_z^{(0)})|_{z_m=0} + v_z^{(4)}|_{z_\mu=0}, \\ v_z^{(4)}|_{z_\mu=0} &= \frac{\partial \eta^{(4)}}{\partial t} + \alpha \left(u_x^{(0)} \frac{\partial \eta^{(2)}}{\partial x_m} + \mathbf{u}^{(0)} \cdot \nabla \eta^{(1)} \right)|_{z_m=0}. \end{aligned} \quad (3.40)$$

Now, we use ${}^m(\text{Inc})^3$ in (3.9), namely $\text{div} \mathbf{u}^{(3)} + \text{div}_m \mathbf{u}^{(4)} = 0$, that we integrate over Ω . By doing so and accounting for the boundary condition ${}^m(\text{RC})^4$ in (3.9), we obtain

$$S \text{div} \mathbf{U}^{(3)} + \int_{X_m} u_z^{(4)}(\mathbf{r}, x_m, 0, t) \, dx_m = 0. \quad (3.41)$$

To deduce $u_z^{(4)}|_{z_m=0}$, we extend the matching condition (3.16) at the fourth order, namely

$$u_z^{(4)}|_{z_m=0} = \lim_{z_\mu \rightarrow -\infty} \left(v_z^{(4)} - \alpha(z_\mu + 1) \frac{\partial}{\partial z_m} (\eta^{(1)} u_z^{(1)} + \eta^{(2)} u_z^{(0)})|_{z_m=0} \right). \quad (3.42)$$

Using (3.40), and again ${}^m(\text{Inc})^{0,1}$, we obtain

$$u_z^{(4)}|_{z_m=0} = \frac{\partial \eta^{(4)}}{\partial t} + \alpha \text{div} (\eta^{(1)} \mathbf{u}^{(0)})|_{z_m=0} + \alpha \frac{\partial}{\partial x_m} (\eta^{(2)} u_x^{(0)} + \eta^{(1)} u_x^{(1)})|_{z_m=0} \quad (3.43)$$

(we also used the property that $\eta^{(1)}$ does not depend on x_m from (3.21)). Inserting the above result in (3.41), the integral of the third term of (3.43) vanishes by periodicity, as previously, and with $\eta^{(1)} = \bar{\eta}^{(1)}$ from (3.21), we obtain the second relation in (3.37a).

We now consider the problem satisfied by $(\mathbf{u}^{(3)}, \varphi^{(4)})$ in $\mathbf{r}_m \in \Omega$ coordinate. From ${}^m(\text{Inc})^2$, ${}^m(\text{Rot})^3$, ${}^m(\text{RC})^3$ in (3.9) and with $u_z^{(3)}$ at $z_m = 0$ given by (3.32), the problem reads

$$\left\{ \begin{array}{l} \text{div}_m \mathbf{u}^{(3)} = -\text{div} \mathbf{u}^{(2)}, \quad \mathbf{u}^{(3)} = \nabla_m \varphi^{(4)} + \nabla \varphi^{(3)}, \quad \text{in } \Omega, \\ \mathbf{u}^{(3)} \cdot \mathbf{n} = 0 \text{ on the walls,} \\ u_z^{(3)} = \frac{\partial \eta^{(3)}}{\partial t}(\mathbf{r}, x_m, t) + \alpha \frac{\partial}{\partial x_m} \left(\eta^{(1)}(\mathbf{r}, t) u_x^{(0)}(\mathbf{r}, x_m, 0, t) \right) \text{ at } z_m = 0, \\ \mathbf{u}^{(3)}, \varphi^{(4)} \text{ } p\text{-periodic with respect to } x_m. \end{array} \right. \quad (3.44)$$

We know the expressions for $(\mathbf{u}^{(2)}, \varphi^{(3)})$ from (3.35) and (3.36), $\eta^{(3)}$ from (3.32) and (3.29), $\eta^{(1)}$ from (3.20) and (3.21) and $u_x^{(0)}$ from (3.23). This static problem can be decomposed as a linear combination of the macroscopic components $\partial_x \bar{\varphi}^{(3)}$, $(\partial_{xx} \bar{\varphi}^{(2)}, \partial_{yy} \bar{\varphi}^{(2)})$ and $(\partial_{xxx} \bar{\varphi}^{(1)}, \partial_{xyy} \bar{\varphi}^{(1)})$ in a similar way to the previous order, see (3.36). The additional macroscopic components compared with the previous order are the fourth-order derivatives $(\partial_{xxxx} \bar{\varphi}^{(0)}, \partial_{xxyy} \bar{\varphi}^{(0)}, \partial_{yyyy} \bar{\varphi}^{(0)})$ as well as the nonlinear term $\alpha \bar{\eta}^{(1)} (\partial \bar{\varphi}^{(0)} / \partial x)$ (see Appendix A.2). Accordingly, we set

$$\begin{aligned} \varphi^{(4)} &= \bar{\varphi}^{(4)} + \frac{\partial \bar{\varphi}^{(3)}}{\partial x} Q^{(0)} + \frac{\partial^2 \bar{\varphi}^{(2)}}{\partial x^2} Q_x^{(1)} + \frac{\partial^2 \bar{\varphi}^{(2)}}{\partial y^2} Q_y^{(1)} + \frac{\partial^3 \bar{\varphi}^{(1)}}{\partial x^3} Q_x^{(2)} + \frac{\partial^3 \bar{\varphi}^{(1)}}{\partial x \partial y^2} Q_y^{(2)}, \\ &+ \frac{\partial^4 \bar{\varphi}^{(0)}}{\partial x^4} Q_x^{(3)} + \frac{\partial^4 \bar{\varphi}^{(0)}}{\partial x^2 \partial y^2} Q_{xy}^{(3)} + \frac{\partial^4 \bar{\varphi}^{(0)}}{\partial y^4} Q_y^{(3)} - \alpha \bar{\eta}^{(1)} \frac{\partial \bar{\varphi}^{(0)}}{\partial x} Q^{(3)} \end{aligned} \quad (3.45)$$

(and $\mathbf{u}^{(3)}$ given in [Appendix A.1](#)) with $\bar{\varphi}^{(4)}$ defined in (3.17). The elementary problems satisfied by $(Q_x^{(3)}, Q_y^{(3)}, Q_{xy}^{(3)})$ are collected in [Appendix B.1](#) since we shall not use them. Indeed we only need to know that they are even functions of x_m ; the problem satisfied by $Q^{(3)}$ reads

$$\left\{ \begin{array}{l} \operatorname{div}_m(\nabla_m Q^{(3)}) = 0 \quad \text{in } \Omega, \\ \nabla_m Q^{(3)} \cdot \mathbf{n} = 0 \text{ on the walls,} \\ \frac{\partial Q^{(3)}}{\partial z_m} = -\frac{\partial^2}{\partial x_m^2} Q^{(0)}(x_m, 0), \quad \int_{X_m} Q^{(3)} dx_m = 0, \quad \text{at } z_m = 0, \\ Q^{(3)}, \nabla_m Q^{(3)} p\text{-periodic with respect to } x_m, \end{array} \right. \quad (3.46)$$

and we notice that $Q^{(3)}$ is an odd function of x_m , and in the absence of microstructure $Q^{(0)} = 0$, hence $Q^{(3)} = 0$. Integrating $\mathbf{u}^{(3)} = \nabla_m \varphi^{(4)} + \nabla_m \varphi^{(3)}$ in (3.44) over Ω with (3.36) and (3.45) (see (A1) in [Appendix A.1](#) for the detailed form of $\mathbf{u}^{(3)}$) and eliminating the contributions from odd functions, we obtain the form announced in (3.37b) for $U_y^{(3)}$ and

$$U_x^{(3)} = \alpha_x \frac{\partial \bar{\varphi}^{(3)}}{\partial x} + d_{xx} \frac{\partial^3 \bar{\varphi}^{(1)}}{\partial x^3} + d_{xy} \frac{\partial^3 \bar{\varphi}^{(1)}}{\partial x \partial y^2} - \alpha d \bar{\eta}^{(1)} \frac{\partial \bar{\varphi}^{(0)}}{\partial x}, \quad (3.47)$$

with $d = 1/S \int_{\Omega} (\partial Q^{(3)} / \partial x_m) d\mathbf{r}_m$, and it is shown in [Appendix B.2](#) that $d = \kappa(1 - n_x)$.

3.6. Final model

The final model is obtained by gathering the results from order zero to order three, namely (3.19), (3.30) and (3.37), and considering in a first step the unique fields $\mathbf{U} = \mathbf{U}^{(0)} + \delta \mathbf{U}^{(1)} + \dots + \delta^3 \mathbf{U}^{(3)}$, $\bar{\eta} = \delta \bar{\eta}^{(1)} + \dots + \delta^4 \bar{\eta}^{(4)}$. We obtain

$$\left\{ \begin{array}{l} \operatorname{div} \mathbf{U} + \frac{\kappa}{\delta} \frac{\partial \bar{\eta}}{\partial t} + \alpha \delta^2 \kappa \operatorname{div}(\bar{\eta} \nabla \bar{\varphi}) = 0, \\ \frac{\partial \bar{\varphi}}{\partial t} + \frac{1}{\delta} \bar{\eta} + \frac{\alpha \delta^3}{2} \left(n_x \left(\frac{\partial \bar{\varphi}}{\partial x} \right)^2 + \left(\frac{\partial \bar{\varphi}}{\partial y} \right)^2 \right) = 0, \end{array} \right. \quad (3.48a)$$

$$\left\{ \begin{array}{l} U_x = \alpha_x \frac{\partial \bar{\varphi}}{\partial x} + \delta^2 d_{xx} \frac{\partial^3 \bar{\varphi}}{\partial x^3} + \delta^2 d_{xy} \frac{\partial^3 \bar{\varphi}}{\partial x \partial y^2} - \alpha \delta^2 \kappa (1 - n_x) \bar{\eta} \frac{\partial \bar{\varphi}}{\partial x}, \\ U_y = \frac{\partial \bar{\varphi}}{\partial y} + \delta^2 d_{yx} \frac{\partial^3 \bar{\varphi}}{\partial x^2 \partial y} + \delta^2 d_{yy} \frac{\partial^3 \bar{\varphi}}{\partial y^3}. \end{array} \right. \quad (3.48b)$$

By using the velocity at the free surface, $\bar{\mathbf{u}} = \nabla \bar{\varphi}$, instead of \mathbf{U} , and eliminating $\bar{\varphi}$, we obtain

$$\begin{aligned} & \frac{\partial \bar{\eta}}{\partial t} + \delta \operatorname{div} \left[\left(\frac{\alpha_x}{\kappa} + \varepsilon n_x \bar{\eta} \right) \bar{u}_x \mathbf{e}_x + \left(\frac{1}{\kappa} + \varepsilon \bar{\eta} \right) \bar{u}_y \mathbf{e}_y \right] \\ & + \frac{\delta^3}{\kappa} \operatorname{div} \left[\left(d_{xx} \frac{\partial^2 \bar{u}_x}{\partial x^2} + d_{xy} \frac{\partial^2 \bar{u}_x}{\partial y^2} \right) \mathbf{e}_x + \left(d_{yx} \frac{\partial^2 \bar{u}_y}{\partial x^2} + d_{yy} \frac{\partial^2 \bar{u}_y}{\partial y^2} \right) \mathbf{e}_y \right] = 0, \end{aligned} \quad (3.49)$$

$$\begin{aligned} & \frac{\partial \bar{\eta}}{\partial x} + \delta \frac{\partial \bar{u}_x}{\partial t} + \frac{\varepsilon \delta^2}{2} \frac{\partial}{\partial x} \left(n_x \bar{u}_x^2 + \bar{u}_y^2 \right) = 0, \quad \frac{\partial \bar{\eta}}{\partial y} + \delta \frac{\partial \bar{u}_y}{\partial t} + \frac{\varepsilon \delta^2}{2} \frac{\partial}{\partial y} \left(n_x \bar{u}_x^2 + \bar{u}_y^2 \right) = 0, \end{aligned} \quad (3.50)$$

whose dimensional form is given in (2.7), with $\bar{h} = h/\kappa$ being the mean water depth.

4. Analysis of the effective model

We investigate in this section the physical properties of the effective Boussinesq (2.7) and the KdV (2.8), as well as the soliton solution (2.10). To simplify the analysis, we consider a bathymetry composed of plates with vanishing thickness. By doing so, the average water depth $\bar{h} = h$ remains fixed, leaving us with two dimensionless geometrical parameters: the array periodicity rescaled by the water depth column, p , and the rescaled reduced water depth ξ ($\xi = 1$ corresponds to a flat bathymetry). We will see that, in the considered limit of thin plates, the Boussinesq and KdV equations are significantly modified for wave propagation along the x -direction, while they remain unchanged for propagation along the y -direction. The case of oblique propagation continuously varies between these two extremes. This configuration also highlights a potential issue when applying homogenization directly to a reduced problem, written solely in horizontal variables and involving the depth profile $h(x)$ (Quezada de Luna & Ketcheson 2021; Ketcheson *et al.* 2025). In such an approach, if one simply considers a laminated depth profile $h(x)$ that alternates between h and ξh over plates of vanishing thickness, one would incorrectly conclude using homogenization that these plates have no effect on wave propagation – which is not physically accurate in the x -direction.

4.1. Analysis of the anisotropic Boussinesq (2.7)

According to (2.7), the effect of the bathymetry is encapsulated in the parameters (α_x, n_x, d_{xx}) . For a solution depending only on x , (2.7) simplifies to

$$\begin{cases} \frac{\partial \bar{\eta}}{\partial t} + \alpha_x h \frac{\partial \bar{u}_x}{\partial x} + n_x \frac{\partial}{\partial x} \bar{\eta} \bar{u}_x + h^3 d_{xx} \frac{\partial^3 \bar{u}_x}{\partial x^3} = 0, \\ \frac{\partial \bar{u}_x}{\partial t} + g \frac{\partial \bar{\eta}}{\partial x} + n_x \bar{u}_x \frac{\partial \bar{u}_x}{\partial x} = 0, \end{cases} \quad (4.1)$$

and for a flat bathymetry, we have $\alpha_x = n_x = 1$ et $d_{xx} = 1/3$. In contrast, for a solution depending only on y , (2.7) simplifies to

$$\begin{cases} \frac{\partial \bar{\eta}}{\partial t} + h \frac{\partial \bar{u}_y}{\partial y} + \frac{\partial}{\partial y} \bar{\eta} \bar{u}_y + h^3 d_{yy} \frac{\partial^3 \bar{u}_y}{\partial y^3} = 0, \\ \frac{\partial \bar{u}_y}{\partial t} + g \frac{\partial \bar{\eta}}{\partial y} + \bar{u}_y \frac{\partial \bar{u}_y}{\partial y} = 0, \end{cases} \quad (4.2)$$

which differs from the one-dimensional version of (2.4) for a flat bathymetry only in the value of d_{yy} and its deviation from $1/3$. The coefficients (d_{xy}, d_{yx}) appear only for oblique propagation in the (x, y) plane.

Figures 4 and 5 show the variations of the six non-dimensional effective parameters, namely (α_x, n_x) and $(d_{xx}, d_{xy}, d_{yx}, d_{yy})$, which enter effective Boussinesq equations (2.7), see also (4.1) and (4.2). These parameters, defined by (2.12) and (2.13), were obtained by numerically solving, with COMSOL Multiphysics, the potential flow problems given in (2.11) together with table 1. In the numerical set-up, we considered an elementary unit cell (in dimensionless coordinates) of width p and height 1, containing a plate of thickness 10^{-3} and height $(1 - \xi)$.

The deviation of α_x from 1 directly reflects the anisotropy of the medium, which applies both in the linear and nonlinear regimes: it quantifies the ratio of effective water depths in the x - and y -directions. In Maurel *et al.* (2017), it was shown that anisotropy is maximized for infinitely thin plates, which is the case we consider here, and for small spacing p . We recover this result with $\alpha_x \rightarrow \xi$ in the limit $p \rightarrow 0$ (see table 3), meaning that the

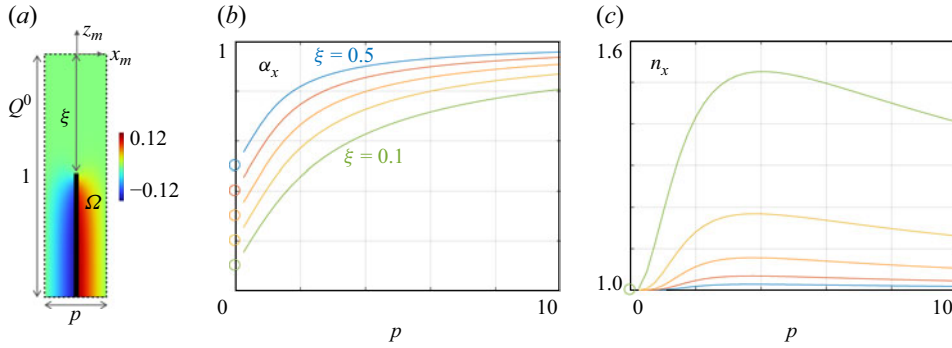


Figure 4. Parameters (α_x, n_x) entering the effective Boussinesq (2.7): (a) $Q^{(0)}(x_m, z_m)$ solution to (2.11) and table 1 ($\xi = 0.5$, $p = 0.25$); (b) (α_x, n_x) against the rescaled periodicity p for increasing rescaled water depth over the plate $\xi = 0.1$ to 0.5 , with a step of 0.1 .

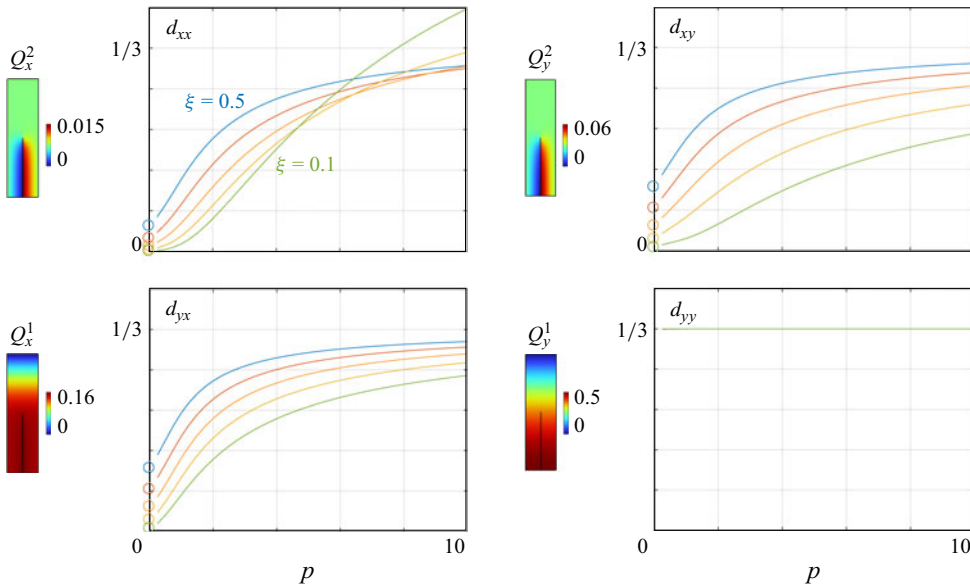


Figure 5. Parameters $(d_{xx}, d_{xy}, d_{yx}, d_{yy})$ entering the effective Boussinesq (2.7) against the rescaled periodicity p for rescaled water depth over the plate $\xi = 0.1$ to 0.5 with a step of 0.1 . The insets show the solutions to the elementary problems in the unit cell for $p = 0.25$ and $\xi = 0.5$.

effective height in the x -direction tends to (ξh) , the smallest water depth imposed by the bathymetry. This result is intuitive since, when the spacing between plates is very small, the flow cannot penetrate the dense vertical layer region, which thus behaves like a flat bottom at depth ξh . This intuitive picture is in line with the analysis presented in Nachbin (2003), see in particular figures 5.1 and 6.2 of that reference. The effective height in the y -direction remains h , the largest water depth imposed by the bathymetry. For infinitely thin plates, this is also intuitive since the flow in the y -direction does not ‘see’ the plates regardless of the periodicity p , at least in the inviscid regime, and thus, only experiences the water column of depth h .

Elementary solutions		Effective parameters
$z_m \in (-1, -\xi)$	$z_m \in (-\xi, 0)$	(2.12)–(2.13)
$Q^{(0)} \simeq \frac{p}{2} - x_m,$	$Q^{(0)}(r_m) \simeq 0$	$\alpha_x \simeq \xi, n_x \simeq 1,$
$Q_x^{(1)} \simeq \frac{1}{2}(x_m^2 - px_m + \xi^2),$	$Q_x^{(1)} \simeq -\frac{z_m^2}{2} - \xi z_m,$	$d_{yx} \simeq \frac{\xi^2}{6}(3 - \xi),$
$Q_y^{(1)} \simeq -\frac{z_m^2}{2} - z_m,$	$Q_y^{(1)} \simeq -\frac{z_m^2}{2} - z_m,$	$d_{yy} \simeq \frac{1}{3},$
$Q_x^{(2)} \simeq -\frac{x_m - \frac{p}{2}}{6} \left(\left(x_m - \frac{p}{2} \right)^2 + 3\xi^2 \right),$	$Q_x^{(2)} \simeq 0,$	$d_{xx} \simeq \frac{\xi^3}{3},$
$Q_y^{(2)} \simeq -\frac{x_m - \frac{p}{2}}{6} \left(\left(x_m - \frac{p}{2} \right)^2 + 3(z_m^2 + 2z_m) \right),$	$Q_y^{(2)} \simeq 0,$	$d_{xy} \simeq \frac{\xi^2}{6}(3 - \xi),$

Table 3. Estimates of the effective parameters for flat bathymetry in the limit of small periodicity to water depth ratio p .

In the considered range of plate heights, variations in the nonlinearity parameter n_x are relatively small, deviating only slightly from the value 1 corresponding to a flat bathymetry. Turning to the dispersion parameters, as mentioned earlier and as expected for infinitely thin plates, $d_{yy} \approx 1/3$ regardless of p and ξ . The numerical computation of d_{yy} retrieves this theoretical value with an accuracy of 0.3 %. In comparison, the dispersion parameters (d_{xx} , d_{xy} , d_{yx}) decrease significantly as p and ξ decrease. Notably, the effective heights $\alpha_x h$ and $(3d_{xx})^{1/3}h$ coincide only for small values of p .

These variations indicate that wave propagation along y is unaffected by the presence of plates. In contrast, when the array is dense ($p \rightarrow 0$), wave propagation along x corresponds to propagation over the smallest water depth ξh imposed by the bathymetry, with $\alpha_x h = \xi h$, $d_{xx}h^3 = (1/3)(\xi h)^3$ and $n_x = 1$ in (4.1).

4.2. Analysis of the anisotropic KdV equation (2.8) and associated soliton solutions

We start by analysing the KdV equation. For wave propagation along x ($\theta = 0$), (2.8) combined with (2.9) gives

$$\frac{\partial \bar{\eta}}{\partial t} + c_0 \left(1 + \frac{3}{2} \frac{\bar{\eta}}{h_0} \right) \frac{\partial \bar{\eta}}{\partial x} + \gamma_0 \frac{c_0 h_0^2}{6} \frac{\partial^3 \bar{\eta}}{\partial x^3} = 0, \quad c_0 = \sqrt{g H_0}, \quad (4.3)$$

where

$$H_0 = \alpha_x h, \quad h_0 = \frac{\alpha_x h}{n_x}, \quad \gamma_0 = \frac{3d_{xx}}{\alpha_x^3} n_x^2. \quad (4.4)$$

This equation differs from (2.5), which holds for a flat bathymetry, in two aspects: the relationship between c_0 and h_0 , since $H_0 \neq h_0$ in general, and the introduction of the coefficient γ_0 , which deviates from unity. As a result, a potential imbalance between the dispersion and nonlinear terms arises. For wave propagation along y , using $h_{(\pi/2)} = h$ and $\gamma_{(\pi/2)} = 3d_{yy} \simeq 1$, we recover the classical KdV equation for a water depth h , as expected.

For the general case of oblique incidence in (2.8), figure 6 displays the variations of the effective depths $(c_\theta/c)^2 = (H_\theta/h)$ in the linear term and (h_θ/h) in the dispersive term as functions of p and θ . The results are shown for $\xi = 0.3$, but aside from bound values, the trends remain similar for different values of ξ . Both effective depths exhibit similar variations, with $H_\theta \geq h_\theta$. In agreement with the Boussinesq equation analysis, equality

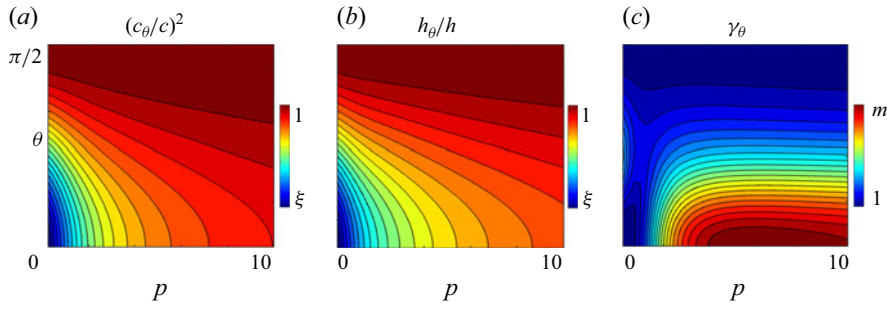


Figure 6. Anisotropic KdV (2.8)–(2.9): variations as functions of p and θ of (a) the normalized effective depths $(c_\theta/c)^2 = (H_\theta/h)$ in the linear terms; (b) h_θ/h in the dispersion; (c) γ_θ in the nonlinear terms. The trends, shown for $\xi = 0.3$ are similar for other values of ξ , with $m \simeq 1 + 0.04(1/\xi^2 - 1)$ representing the maximum of γ_θ obtained for $\theta = 0$.

is reached for $\theta = 0$ and small p ($H_0 = h_0 = \xi h$), as well as for $\theta = \pi/2$ regardless of p ($H_{(\pi/2)} = h_{(\pi/2)} = h$). The parameter γ_θ exceeds 1, reaching its maximum at $\theta = 0$ for intermediate values of p . As ξ decreases, this maximum increases and occurs at larger values of p . Within the considered range of ξ , the maximum is found around $p \sim 5 - 6$ and follows an empirical law of the form $1 + 0.04(1/\xi^2 - 1)$. We refrain from extrapolating the behaviour of the coefficients as $\xi \rightarrow 0$, which would require revisiting the asymptotic analysis. It is worth noting that surface-piercing effects could occur for plates reaching the free surface, which falls beyond the scope of this study.

We now examine the soliton solutions in (2.10), characterized by $\ell_\theta = (4\gamma_\theta h_\theta^3/3\eta_0)^{1/2}$ (its spatial extent) and u_θ (its velocity). The reference case is given by $\ell = (4h^3/3\eta_0)^{1/2}$ and u in (2.6). Consistent with the KdV analysis, the soliton width is maximal for propagation along y , where $\ell_{(\pi/2)} = \ell$, and minimal for propagation along x , with $\ell_0 = \sqrt{(3d_{xx}/n_x)}\ell$. In the limit of dense plate arrays, we obtain $\ell_0 \sim \xi^{3/2}\ell$. To provide a concrete example, we consider a typical configuration with solitons over $h = 10$ cm and $\eta_0 = 0.3h$ (with $g = 9.8$ m s $^{-2}$). Figure 7 presents the variations of these parameters with respect to p for $\theta = 0$ and with respect to θ for $p = 1$. The soliton velocity and exponential tails decrease significantly as p or ξ decreases, to the extent that even for moderate values of ξ , these effects should be experimentally observable. This is illustrated in figure 8, which displays the soliton profiles for $\xi = 0.5, 0.3$ and 0.1 for propagation along x (coloured curves) and along y (grey curves). The profiles are shown at $t = 0$ (solid lines) and $t = 1$ s (dashed lines). Anisotropy in both soliton shape and velocity is already clearly visible for $\xi = 0.5$ and becomes more pronounced as ξ decreases. Note that these profiles correspond to the explicit solutions given in (2.10), rather than to a dynamical solution of the anisotropic KdV (2.8). However, as mentioned earlier, the stability of (2.8) for any propagation direction θ is guaranteed, since it has the same form as the classical KdV equation; therefore, the results of Benjamin (1972) and Bona (1975) apply directly.

5. Concluding remarks

Following the pioneering work of Rosales & Papanicolaou (1983), we have derived effective two-dimensional Boussinesq and KdV equations encapsulating the effect of a periodic, rapidly varying, bathymetry in the x -direction. These equations reveal strong anisotropy, which has been illustrated in the case where the bathymetry results from an array of thin plates, allowing us to explore the effects of the array periodicity and the plate height. Our deliberate choice of a relatively simple geometry, well-grounded in

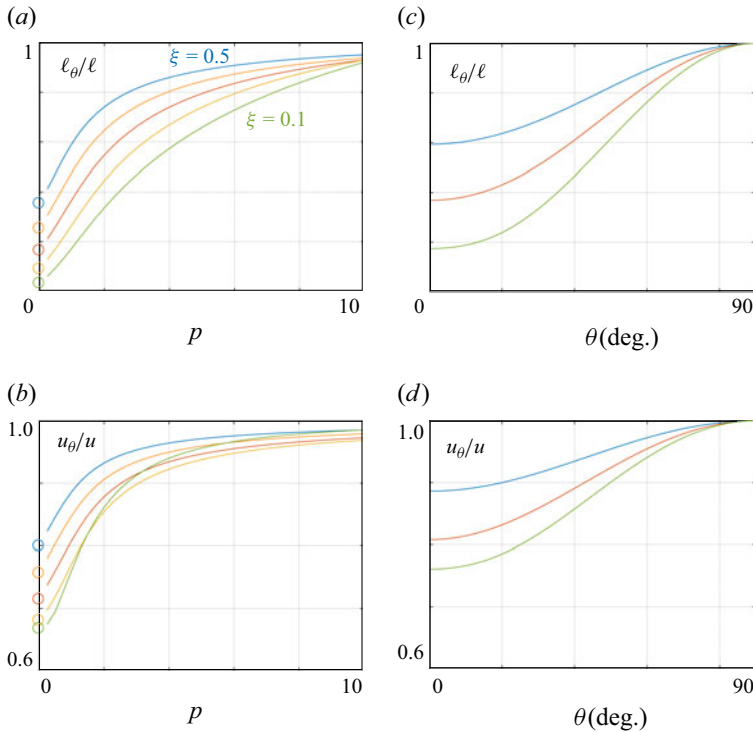


Figure 7. Soliton characteristics: variations of ℓ_θ (spatial extent) and u_θ (velocity) of solitons, (a–b) as functions of p for $\theta = 0$, and (c–d) as functions of θ for $p = 1$. The parameters are set to $h = 0.1$ m and $\eta_0 = 0.03$ m.

the metamaterials literature and easily realizable in a laboratory experiment (Berraquero *et al.* 2013; Maurel *et al.* 2017), enables us to emphasize effective parameters that remain robust in any configuration, as opposed to terms arising only from symmetry breaking. This simplification provides a clear foundation from which extensions to more complex bathymetries can be pursued within the same theoretical framework, with new terms naturally identified and their influence assessed. It also highlights the necessity of considering the three-dimensional effects of the original problem: any homogenization analysis starting from a reduced formulation based solely on a depth profile $h(x)$ fails to capture the plate-induced effects in the limit of vanishing thickness. Altogether, this emphasizes both the theoretical importance and the experimental feasibility of our approach.

The next step is to perform laboratory experiments, to confirm our results by investigating the ability of soliton-like solutions to propagate according to the derived laws and to explore the limitations of the approach, in particular the influence of vortex structures expected to be generated by the plates. From a numerical perspective, the stability of different formulations of the Boussinesq equation has been discussed in the case of a flat bottom, see for example Chen (1998) and Bona *et al.* (2002). A similar discussion can be carried out for the homogenized (2.7) we have obtained. Another promising direction would be to compare our homogenized results, for instance (2.10), with direct numerical simulations in the presence of bathymetry. In particular, the recent work of Svård & Kalisch (2025) is highly relevant, as it establishes a Boussinesq system

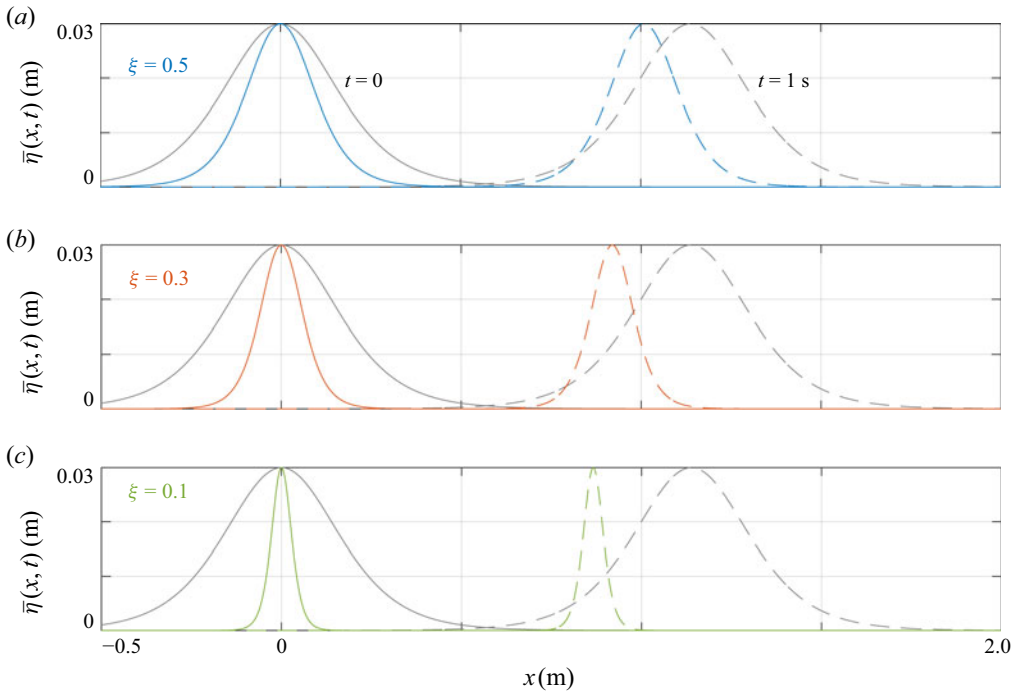


Figure 8. Soliton profiles $\bar{\eta}(x, t)$ propagating along x ($\theta = 0$), shown at $t = 0$ (solid coloured lines) and $t = 1$ s (dashed coloured lines), obtained from (2.10) for (a) $\xi = 0.5$, (b) $\xi = 0.3$ and (c) $\xi = 0.1$. The grey curves represent the reference solution $\eta(x, t)$ from (2.6), which corresponds to propagation along y , i.e. $\bar{\eta}(y, t)$.

that is numerically stable even in the case of discontinuous bathymetries, including step configurations. This suggests a natural opportunity to confront the predictions of our homogenized model with those obtained from direct simulations over stepped bathymetries.

Acknowledgements. A.M. and K.P. gratefully acknowledge the hospitality of Kyoto University (Hakubi Center for Advanced Research and the Disaster Prevention Research Institute during their visit in August 2023), as well as the Okinawa Institute of Science and Technology (Marine Physics and Engineering Unit during their stay in June 2025), where part of this work was carried out in collaboration with A.C.

Funding. A.M. acknowledges support from the French National Research Agency (ANR) under grant no. ANR-21-CE30-0046 (CoProMM), and K.P. acknowledges support from the ANR under grant no. ANR-19-CE08-0006 (MetaReso). A.C. acknowledges support from the Okinawa Institute of Science and Technology (OIST) with subsidy funding from the Cabinet Office, Government of Japan.

Declaration of interests. The authors report no conflict of interest.

Appendix A. Additional results for the asymptotic procedure

A.1. The velocities $\mathbf{u}^{(n)}$

In this section, we provide the expressions of the velocities $\mathbf{u}^{(n)} = \nabla_m \varphi^{(n+1)} + \nabla \varphi^{(n)}$ (from ${}^m(\text{Rot})^n$ in (3.9)), the integration of which over Ω provides $\mathbf{U}^{(n)}$ defined in (3.17). We have determined $\varphi^{(n)}$, $n = -1, \dots, 3$ in (3.20), (3.24), (3.29), (3.36) and (3.45).

For completeness, we provide below the forms of $\mathbf{u}^{(n)}$ for $n = 0, 1, 2, 3$ given, respectively, by (3.23) (3.28), (3.35) and (3.44). Specifically, we obtain

$$\begin{aligned}
 \mathbf{u}^{(0)} &= \frac{\partial \bar{\varphi}^{(0)}}{\partial x} (\nabla_m \mathcal{Q}^{(0)} + \mathbf{e}_x) + \frac{\partial \bar{\varphi}^{(0)}}{\partial y} \mathbf{e}_y, \\
 \mathbf{u}^{(1)} &= \frac{\partial \bar{\varphi}^{(1)}}{\partial x} (\nabla_m \mathcal{Q}^{(0)} + \mathbf{e}_x) + \frac{\partial \bar{\varphi}^{(1)}}{\partial y} \mathbf{e}_y \\
 &\quad + \frac{\partial^2 \bar{\varphi}^{(0)}}{\partial x^2} (\nabla_m \mathcal{Q}_x^{(1)} + \mathcal{Q}^{(0)} \mathbf{e}_x) + \frac{\partial^2 \bar{\varphi}^{(0)}}{\partial y^2} \nabla_m \mathcal{Q}_y^{(1)} + \frac{\partial^2 \bar{\varphi}^{(0)}}{\partial x \partial y} \mathcal{Q}^{(0)} \mathbf{e}_y, \\
 \mathbf{u}^{(2)} &= \frac{\partial \bar{\varphi}^{(2)}}{\partial x} (\nabla_m \mathcal{Q}^{(0)} + \mathbf{e}_x) + \frac{\partial \bar{\varphi}^{(2)}}{\partial y} \mathbf{e}_y \\
 &\quad + \frac{\partial^2 \bar{\varphi}^{(1)}}{\partial x^2} (\nabla_m \mathcal{Q}_x^{(1)} + \mathcal{Q}^{(0)} \mathbf{e}_x) + \frac{\partial^2 \bar{\varphi}^{(1)}}{\partial y^2} \nabla_m \mathcal{Q}_y^{(1)} + \frac{\partial^2 \bar{\varphi}^{(1)}}{\partial x \partial y} \mathcal{Q}^{(0)} \mathbf{e}_y \\
 &\quad + \frac{\partial^3 \bar{\varphi}^{(0)}}{\partial x^3} (\nabla_m \mathcal{Q}_x^{(2)} + \mathcal{Q}_x^{(1)} \mathbf{e}_x) + \frac{\partial^3 \bar{\varphi}^{(0)}}{\partial x \partial y^2} (\nabla_m \mathcal{Q}_y^{(2)} + \mathcal{Q}_y^{(1)} \mathbf{e}_x) \\
 &\quad + \frac{\partial^3 \bar{\varphi}^{(0)}}{\partial x^2 \partial y} \mathcal{Q}_x^{(1)} \mathbf{e}_y + \frac{\partial^3 \bar{\varphi}^{(0)}}{\partial y^3} \mathcal{Q}_y^{(1)} \mathbf{e}_y, \\
 \mathbf{u}^{(3)} &= \frac{\partial \bar{\varphi}^{(3)}}{\partial x} (\nabla_m \mathcal{Q}^{(0)} + \mathbf{e}_x) + \frac{\partial \bar{\varphi}^{(3)}}{\partial y} \mathbf{e}_y \\
 &\quad + \frac{\partial^2 \bar{\varphi}^{(2)}}{\partial x^2} (\nabla_m \mathcal{Q}_x^{(1)} + \mathcal{Q}^{(0)} \mathbf{e}_x) + \frac{\partial^2 \bar{\varphi}^{(2)}}{\partial y^2} \nabla_m \mathcal{Q}_y^{(1)} + \frac{\partial^2 \bar{\varphi}^{(2)}}{\partial x \partial y} \mathcal{Q}^{(0)} \mathbf{e}_y \\
 &\quad + \frac{\partial^3 \bar{\varphi}^{(1)}}{\partial x^3} (\nabla_m \mathcal{Q}_x^{(2)} + \mathcal{Q}_x^{(1)} \mathbf{e}_x) + \frac{\partial^3 \bar{\varphi}^{(1)}}{\partial x \partial y^2} (\nabla_m \mathcal{Q}_y^{(2)} + \mathcal{Q}_y^{(1)} \mathbf{e}_x) \\
 &\quad + \frac{\partial^3 \bar{\varphi}^{(1)}}{\partial x^2 \partial y} \mathcal{Q}_x^{(1)} \mathbf{e}_y + \frac{\partial^3 \bar{\varphi}^{(1)}}{\partial y^3} \mathcal{Q}_y^{(1)} \mathbf{e}_y \\
 &\quad + \frac{\partial^4 \bar{\varphi}^{(0)}}{\partial x^4} (\nabla_m \mathcal{Q}_x^{(3)} + \mathcal{Q}_x^{(2)} \mathbf{e}_x) + \frac{\partial^4 \bar{\varphi}^{(0)}}{\partial x^2 \partial y^2} (\nabla_m \mathcal{Q}_{xy}^{(3)} + \mathcal{Q}_y^{(2)} \mathbf{e}_x) + \frac{\partial^4 \bar{\varphi}^{(0)}}{\partial y^4} \nabla_m \mathcal{Q}_y^{(3)} \\
 &\quad - \alpha \frac{\partial \bar{\varphi}^{(0)}}{\partial x} \bar{\eta}^{(1)} \nabla_m \mathcal{Q}^{(3)} + \frac{\partial^4 \bar{\varphi}^{(0)}}{\partial x^3 \partial y} \mathcal{Q}_x^{(2)} \mathbf{e}_y + \frac{\partial^4 \bar{\varphi}^{(0)}}{\partial x \partial y^3} \mathcal{Q}_y^{(2)} \mathbf{e}_y. \tag{A1}
 \end{aligned}$$

A.2. The linearity of problems (3.23), (3.28), (3.35) and (3.44)

Part of the analysis consists in decomposing cell problems (3.23), (3.28), (3.35) and (3.44) satisfied by $(\mathbf{u}^{(n)}, \varphi^{(n+1)})$, $n = 0, \dots, 3$ into linear elementary problems in terms of $\mathbf{r}_m \in \Omega$ coordinate. To do so, we identify independent external sources which are function of the macroscopic space variable and time variable (\mathbf{r}, t) only (not of \mathbf{r}_m). For $n = 0$, this is rather simple since (3.23) appears to be linear with respect to the external sources being the two components of $\nabla \bar{\varphi}^{(0)}$, which provides $\varphi^{(1)}$ in (3.24) and $\mathbf{u}^{(0)}$ in (A1). For $n \geq 1$, we need to identify the macroscopic sources in the quantities $\text{div} \mathbf{u}^{(n-1)}$, $\nabla \varphi^{(n)}$ and $u_z^{(n)}$ at $z_m = 0$ that appear in the cell problems (3.23), (3.28), (3.35) and (3.44). These quantities can be explicitly computed from the previous order $(n - 1)$. For completeness, we provide

below the forms of these quantities in terms of the macroscopic sources. For the $\text{div} \mathbf{u}^{(n-1)}$ with $n = 1, 2, 3$, exploiting (A1), we get

$$\begin{aligned}\text{div} \mathbf{u}^{(0)} &= \frac{\partial^2 \bar{\varphi}^{(0)}}{\partial x^2} \left(\frac{\partial Q^{(0)}}{\partial x_m} + 1 \right) + \frac{\partial^2 \bar{\varphi}^{(0)}}{\partial y^2}, \\ \text{div} \mathbf{u}^{(1)} &= \frac{\partial^2 \bar{\varphi}^{(1)}}{\partial x^2} \left(\frac{\partial Q^{(0)}}{\partial x_m} + 1 \right) + \frac{\partial^2 \bar{\varphi}^{(1)}}{\partial y^2} \\ &\quad + \frac{\partial^3 \bar{\varphi}^{(0)}}{\partial x^3} \left(\frac{\partial Q_x^{(1)}}{\partial x_m} + Q^{(0)} \right) + \frac{\partial^3 \bar{\varphi}^{(0)}}{\partial x \partial y^2} \left(\frac{\partial Q_y^{(1)}}{\partial x_m} + Q^{(0)} \right), \\ \text{div} \mathbf{u}^{(2)} &= \frac{\partial^2 \bar{\varphi}^{(2)}}{\partial x^2} \left(\frac{\partial Q^{(0)}}{\partial x_m} + 1 \right) + \frac{\partial^2 \bar{\varphi}^{(2)}}{\partial y^2} \\ &\quad + \frac{\partial^3 \bar{\varphi}^{(1)}}{\partial x^3} \left(\frac{\partial Q_x^{(1)}}{\partial x_m} + Q^{(0)} \right) + \frac{\partial^3 \bar{\varphi}^{(1)}}{\partial x \partial y^2} \left(\frac{\partial Q_y^{(1)}}{\partial x_m} + Q^{(0)} \right) \\ &\quad + \frac{\partial^4 \bar{\varphi}^{(0)}}{\partial x^4} \left(\frac{\partial Q_x^{(2)}}{\partial x_m} + Q_x^{(1)} \right) + \frac{\partial^4 \bar{\varphi}^{(0)}}{\partial x^2 \partial y^2} \left(\frac{\partial Q_y^{(2)}}{\partial x_m} + Q_x^{(1)} + Q_y^{(1)} \right) + \frac{\partial^4 \bar{\varphi}^{(0)}}{\partial y^4} Q_y^{(1)}.\end{aligned}\tag{A2}$$

Next, for $\varphi^{(n)}$ with $n = 1, 2, 3$, using (3.24), (3.29) and (3.36), we obtain

$$\begin{aligned}\nabla \varphi^{(1)} &= \nabla \bar{\varphi}^{(1)} + \left(\frac{\partial^2 \bar{\varphi}^{(0)}}{\partial x^2} \mathbf{e}_x + \frac{\partial^2 \bar{\varphi}^{(0)}}{\partial x \partial y} \mathbf{e}_y \right) Q^{(0)}, \\ \nabla \varphi^{(2)} &= \nabla \bar{\varphi}^{(2)} + \left(\frac{\partial^2 \bar{\varphi}^{(1)}}{\partial x^2} \mathbf{e}_x + \frac{\partial^2 \bar{\varphi}^{(1)}}{\partial x \partial y} \mathbf{e}_y \right) Q^{(0)} \\ &\quad + \left(\frac{\partial^3 \bar{\varphi}^{(0)}}{\partial x^3} Q_x^{(1)} + \frac{\partial^3 \bar{\varphi}^{(0)}}{\partial x \partial y^2} Q_y^{(1)} \right) \mathbf{e}_x + \left(\frac{\partial^3 \bar{\varphi}^{(0)}}{\partial x^2 \partial y} Q_x^{(1)} + \frac{\partial^3 \bar{\varphi}^{(0)}}{\partial y^3} Q_y^{(1)} \right) \mathbf{e}_y, \\ \nabla \varphi^{(3)} &= \nabla \bar{\varphi}^{(3)} + \left(\frac{\partial^2 \bar{\varphi}^{(2)}}{\partial x^2} \mathbf{e}_x + \frac{\partial^2 \bar{\varphi}^{(2)}}{\partial x \partial y} \mathbf{e}_y \right) Q^{(0)} \\ &\quad + \left(\frac{\partial^3 \bar{\varphi}^{(1)}}{\partial x^3} Q_x^{(1)} + \frac{\partial^3 \bar{\varphi}^{(1)}}{\partial x \partial y^2} Q_y^{(1)} \right) \mathbf{e}_x + \left(\frac{\partial^3 \bar{\varphi}^{(1)}}{\partial x^2 \partial y} Q_x^{(1)} + \frac{\partial^3 \bar{\varphi}^{(1)}}{\partial y^3} Q_y^{(1)} \right) \mathbf{e}_y \\ &\quad + \left(\frac{\partial^4 \bar{\varphi}^{(0)}}{\partial x^4} Q_x^{(2)} + \frac{\partial^4 \bar{\varphi}^{(0)}}{\partial x^2 \partial y^2} Q_y^{(2)} \right) \mathbf{e}_x + \left(\frac{\partial^4 \bar{\varphi}^{(0)}}{\partial x^3 \partial y} Q_x^{(2)} + \frac{\partial^4 \bar{\varphi}^{(0)}}{\partial x \partial y^3} Q_y^{(2)} \right) \mathbf{e}_y.\end{aligned}\tag{A3}$$

Eventually, $u_z^{(n)}$ at $z_m = 0$ for $n = 1, 2, 3$, and using that $\partial_{tt} \bar{\varphi}^{(n)} = 1/\kappa (\alpha_x \partial_{xx} \bar{\varphi}^{(n)} + \partial_{yy} \bar{\varphi}^{(n)})$, $n = 0, 1$, from (3.19a)–(3.19b), we also have

$$\begin{aligned}
 u_z^{(1)}|_{z_m=0} &= -\frac{1}{\kappa} \left(\alpha_x \frac{\partial^2 \bar{\varphi}^{(0)}}{\partial x^2} + \frac{\partial^2 \bar{\varphi}^{(0)}}{\partial y^2} \right), \\
 u_z^{(2)}|_{z_m=0} &= -\frac{1}{\kappa} \left(\alpha_x \frac{\partial^2 \bar{\varphi}^{(1)}}{\partial x^2} + \frac{\partial^2 \bar{\varphi}^{(1)}}{\partial y^2} \right) - \frac{1}{\kappa} \frac{\partial}{\partial x} \left(\alpha_x \frac{\partial^2 \bar{\varphi}^{(0)}}{\partial x^2} + \frac{\partial^2 \bar{\varphi}^{(0)}}{\partial y^2} \right) Q^{(0)}|_{z_m=0}, \\
 u_z^{(3)}|_{z_m=0} &= -\frac{1}{\kappa} \left(\alpha_x \frac{\partial^2 \bar{\varphi}^{(2)}}{\partial x^2} + \frac{\partial^2 \bar{\varphi}^{(2)}}{\partial y^2} + d_{xx} \frac{\partial \bar{\varphi}^{(0)}}{\partial x^4} + (d_{xy} + d_{yx}) \frac{\partial \bar{\varphi}^{(0)}}{\partial x^2 \partial y^2} + d_{yy} \frac{\partial \bar{\varphi}^{(0)}}{\partial y^4} \right) \\
 &\quad - \frac{1}{\kappa} \frac{\partial}{\partial x} \left(\alpha_x \frac{\partial^2 \bar{\varphi}^{(1)}}{\partial x^2} + \frac{\partial^2 \bar{\varphi}^{(1)}}{\partial y^2} \right) Q^{(0)}|_{z_m=0} \\
 &\quad - \frac{1}{\kappa} \frac{\partial^2}{\partial x^2} \left(\alpha_x \frac{\partial^2 \bar{\varphi}^{(0)}}{\partial x^2} + \frac{\partial^2 \bar{\varphi}^{(0)}}{\partial y^2} \right) Q_x^{(1)}|_{z_m=0} \\
 &\quad - \frac{1}{\kappa} \frac{\partial^2}{\partial y^2} \left(\alpha_x \frac{\partial^2 \bar{\varphi}^{(0)}}{\partial x^2} + \frac{\partial^2 \bar{\varphi}^{(0)}}{\partial y^2} \right) Q_y^{(1)}|_{z_m=0} \\
 &\quad - \alpha \frac{\partial \bar{\varphi}^{(0)}}{\partial t} \frac{\partial \bar{\varphi}^{(0)}}{\partial x} \frac{\partial^2 Q^{(0)}}{\partial x_m^2} \Big|_{z_m=0}. \tag{A4}
 \end{aligned}$$

From the expansions of $(\operatorname{div} \mathbf{u}^{(0)}, \nabla \varphi^{(1)}, u_z^{(1)}|_{z_m=0})$ with respect to the macroscopic sources, we deduce from (3.28) by linearity the form $\varphi^{(2)}$ in (3.29) and $\mathbf{u}^{(1)}$ given in (A1). By doing the same with $(\operatorname{div} \mathbf{u}^{(1)}, \nabla \varphi^{(2)}, u_z^{(2)}|_{z_m=0})$, we find from (3.35) the form of $\varphi^{(3)}$ in (3.36) and $\mathbf{u}^{(2)}$ in (A1); and from $(\operatorname{div} \mathbf{u}^{(2)}, \nabla \varphi^{(3)}, u_z^{(3)}|_{z_m=0})$, we obtain from (3.44) the form $\varphi^{(3)}$ in (3.45) and $\mathbf{u}^{(3)}$ in (A1).

Appendix B. The elementary problems at order $n = 3$

B.1. The elementary problems on $Q_x^{(3)}$, $Q_y^{(3)}$ and $Q_{xy}^{(3)}$ in (3.45)

In (3.45), we have introduced four elementary functions satisfying cell problems, among which only $Q^{(3)}$ solving (3.46) is needed at this last order with the others functions being necessary only if we push the expansion to the next orders $n \geq 4$. These elementary functions $(Q_x^{(3)}, Q_y^{(3)}, Q_{xy}^{(3)})$ satisfy the generic cell problem (2.11) with coefficients given in table 4. With $(Q_x^{(1)}, Q_y^{(1)})$ even and $(Q_x^{(2)}, Q_y^{(2)})$ even and odd functions of x_m , respectively, we deduce that $(Q_x^{(3)}, Q_y^{(3)}, Q_{xy}^{(3)})$ are even functions of x_m .

B.2. Relation between d and n_x

The effective parameters d and n_x are defined by

$$d = \frac{1}{S} \int_{\Omega} \frac{\partial Q^{(3)}}{\partial x_m} \, d\mathbf{r}_m, \quad n_x = 1 + \frac{1}{p} \int_{x_m} \left(\frac{\partial Q^{(0)}}{\partial x_m}(x_m, 0) \right)^2 \, dx_m, \tag{B1}$$

with $Q^{(0)}$ satisfying the generic cell problem (2.11) with coefficients (1) and $Q^{(3)}$ satisfying (3.46). Below we establish that $d = \kappa(1 - n_x)$ which is used to obtain that $U_x^{(3)}$

Q :	$Q_x^{(3)}$	$Q_y^{(3)}$	$Q_{xy}^{(3)}$
F :	$Q_x^{(2)}$	0	$Q_y^{(2)}$
G :	$-\left(\frac{\partial Q_x^{(2)}}{\partial x_m} + Q_x^{(1)}\right)$	$-Q_y^{(1)}$	$-\left(\frac{\partial Q_y^{(2)}}{\partial x_m} + Q_x^{(1)} + Q_y^{(1)}\right)$
H :	$-\frac{d_{xx}}{\kappa} - \frac{\alpha_x}{\kappa} Q_x^{(1)} _{z_m=0}$	$-\frac{d_{yy}}{\kappa} - \frac{1}{\kappa} Q_y^{(1)} _{z_m=0}$	$-\frac{d_{xy} + d_{yx}}{\kappa} - \left(\frac{1}{\kappa} Q_x^{(1)} _{z_m=0} + \frac{\alpha_x}{\kappa} Q_y^{(1)} _{z_m=0}\right)$

Table 4. The elementary problems at third order associated with the Poisson type cell problem (2.11). For each elementary problem, we provide the corresponding bulk sources $F(\mathbf{r}_m)$, $G(\mathbf{r}_m)$ and surface source $H(x_m)$.

in (3.37b) and (3.47) are consistent. To do so, we consider the two identities

$$0 = \int_{\Omega} Q^{(3)} \operatorname{div}_m (\nabla_m Q^{(0)} + \mathbf{e}_x) \, d\mathbf{r}_m = \int_{\Omega} \nabla_m Q^{(3)} \cdot \nabla_m Q^{(0)} \, d\mathbf{r}_m - \int_{\Omega} \frac{\partial Q^{(3)}}{\partial x_m} \, d\mathbf{r}_m = Sd, \quad (\text{B2})$$

and

$$0 = \int_{\Omega} Q^{(0)} \operatorname{div}_m (\nabla_m Q^{(3)}) \, d\mathbf{r}_m = \int_{\Omega} \nabla_m Q^{(0)} \cdot \nabla_m Q^{(3)} \, d\mathbf{r}_m - \int_{X_m} Q^{(0)} \frac{\partial Q^{(3)}}{\partial z_m} \, dx_m, \quad (\text{B3})$$

which are obtained by using the divergence theorem together with the periodic conditions and boundary conditions satisfied by $Q^{(0)}$ and $Q^{(3)}$. Applying once again the divergence theorem at the free surface in the right-hand side of (B3) and making use of the periodic conditions satisfied by $Q^{(0)}$ at $x_m = 0$ and $x_m = p$, we get

$$\int_{X_m} -Q^{(0)} \frac{\partial Q^{(3)}}{\partial z_m} \, dx_m = \int_{X_m} Q^{(0)} \frac{\partial^2 Q^{(0)}}{\partial x_m^2} \, dx_m = - \int_{X_m} \left(\frac{\partial Q^{(0)}}{\partial x_m} \right)^2 \, dx_m = p(1 - n_x). \quad (\text{B4})$$

Equating (B2) and (B3) with the help of (B4) gives the announced result.

REFERENCES

- AGNON, Y., MADSEN, P.A. & SCHÄFFER, H.A. 1999 A new approach to high-order Boussinesq models. *J. Fluid Mech.* **399**, 319–333.
- ANDRADE, D. & NACHBIN, A. 2018 Two-dimensional surface wave propagation over arbitrary ridge-like topographies. *SIAM J. Appl. Math.* **78** (5), 2465–2490.
- BEJI, S. & NADAOKA, K. 1996 A formal derivation and numerical modelling of the improved Boussinesq equations for varying depth. *Ocean Engne.* **23** (8), 691–704.
- BENJAMIN, T.B. 1972 The stability of solitary waves. *Proc. Royal Soc. London. A. Math. Phys. Sci.* **328**, 1573, 153–183.
- BERRAQUERO, C.P., MAUREL, A., PETITJEANS, P. & PAGNEUX, V. 2013 Experimental realization of a water-wave metamaterial shifter. *Phys. Rev. E—Statist. Nonlinear Soft Matter Phys.* **88** (5), 051002.
- BOBINSKI, T., EDDI, A., PETITJEANS, P., MAUREL, A. & PAGNEUX, V. 2015 Experimental demonstration of epsilon-near-zero water waves focusing. *Appl. Phys. Lett.* **107** (1).
- BONA, J. 1975 On the stability theory of solitary waves. *Proc. Royal Soc. London. A. Math. Phys. Sci.* **344**(1638), 363–374.
- BONA, J.L., CHEN, M. & SAUT, J.-C. 2002 Boussinesq equations and other systems for small-amplitude long waves in nonlinear dispersive media. i: derivation and linear theory. *J. Nonlinear Sci.* **12**, 283–318.
- BOUSSINESQ, J. 1871 Théorie de l'intumescence liquide appelée onde solitaire ou de translation se propageant dans un canal rectangulaire. *C.R. Acad. Sci. Paris* **72**, 755–759, 1871.
- BROCCHINI, M. 2013 A reasoned overview on Boussinesq-type models: the interplay between physics, mathematics and numerics. *Proc. R. Soc. A.* **469** (2160), 20130496.

- CHEN, M. 1998 Exact traveling-wave solutions to bidirectional wave equations. *Int. J. Theor. Phys.* **37** (5), 1547–1567.
- CRAIG, W., GUYENNE, P., NICHOLLS, D.P. & SULEM, C. 2005 Hamiltonian long-wave expansions for water waves over a rough bottom. *Proc. R. Soc. A.* **461**, 839–873.
- FARHAT, M., ENOCH, S., GUENNEAU, S. & MOVCHAN, A.B. 2008 Broadband cylindrical acoustic cloak for linear surface waves in a fluid. *Phys. Rev. Lett.* **101** (13), 134501.
- GARNIER, J., KRAENKEL, R.A. & NACHBIN, A. 2007 Optimal boussinesq model for shallow-water waves interacting with a microstructure. *Phys. Rev. E* **76** (4), 046311.
- HUA, Y., QIAN, C., CHEN, H. & WANG, H. 2022 Experimental topology-optimized cloak for water waves. *Mater. Today Phys.* **27**, 100754.
- KETCHESON, D.I., LÓCZI, L. & RUSSO, G. 2025 A multiscale model for weakly nonlinear shallow water waves over periodic bathymetry. *Multiscale Model. Sim.* **23** (1), 397–430.
- KLOPMAN, G., VAN GROESEN, B. & DINGEMANS, M.W. 2010 A variational approach to Boussinesq modelling of fully nonlinear water waves. *J. Fluid Mech.* **657**, 36–63.
- KRISHNAN, E.V. 1982 An exact solution of the classical boussinesq equation. *J. Phys. Soc. Japan* **51** (8), 2391–2392.
- LI, C., XU, L., ZHU, L., ZOU, S., LIU, Q.H., WANG, Z. & CHEN, H. 2018 Concentrators for water waves. *Phys. Rev. Lett.* **121** (10), 104501.
- LORENZO, M., PEZZUTTO, P., DE LILLO, F., VENTRELLA, F.M., DE VITA, F., BOSIA, F. & ONORATO, M. 2023 Attenuating surface gravity waves with an array of submerged resonators: an experimental study. *J. Fluid Mech.* **973**, A16.
- QUEZADA DE LUNA, M. & KETCHESON, D.I. 2021 Solitary water waves created by variations in bathymetry. *J. Fluid Mech.* **917**, A45.
- MADSEN, P.A., BINGHAM, H.B. & LIU, H. 2002 A new Boussinesq method for fully nonlinear waves from shallow to deep water. *J. Fluid Mech.* **462**, 1–30.
- MADSEN, P.A., FUHRMAN, D.R. & WANG, B. 2006 A Boussinesq-type method for fully nonlinear waves interacting with a rapidly varying bathymetry. *Coast. Engine.* **53** (5–6), 487–504.
- MADSEN, P.A. & SCHÄFFER, H.A. 1999 A review of Boussinesq-type equations for surface gravity waves. *Adv. Coastal Ocean Engine.* 1–94.
- MADSEN, P.A. & SØRENSEN, O.R. 1992 A new form of the Boussinesq equations with improved linear dispersion characteristics. part 2. A slowly-varying bathymetry. *Coast. Engine.* **18** (3–4), 183–204.
- MARANGOS, C. & PORTER, R. 2021 Shallow water theory for structured bathymetry. *Proc. R. Soc. A.* **477** (2254), 20210421.
- MAUREL, A., MARIGO, J.-J., COBELLI, P., PETITJEANS, P. & PAGNEUX, V. 2017 Revisiting the anisotropy of metamaterials for water waves. *Phys. Rev. B* **96** (13), 134310.
- MAUREL, A., PHAM, K. & MARIGO, J.-J. 2019 Scattering of gravity waves by a periodically structured ridge of finite extent. *J. Fluid Mech.* **871**, 350–376.
- MONSALVE, E., MAUREL, A., PETITJEANS, P. & PAGNEUX, V. 2019 Perfect absorption of water waves by linear or nonlinear critical coupling. *Appl. Phys. Lett.* **114** (1).
- MONSALVE, E., PHAM, K. & MAUREL, A. 2024 Jump conditions for Boussinesq equations due to an abrupt depth transition. *SIAM J. Appl. Math.* **84** (4), 1792–1817.
- NACHBIN, A. 2003 A terrain-following Boussinesq system. *SIAM J. Appl. Math.* **63** (3), 905–922.
- PORTER, R. & NEWMAN, J.N. 2014 Cloaking of a vertical cylinder in waves using variable bathymetry. *J. Fluid Mech.* **750**, 124–143.
- ROSALES, R.R. & PAPANICOLAOU, G.C. 1983 Gravity waves in a channel with a rough bottom. *Stud. Appl. Math.* **68** (2), 89–102.
- SVÄRD, M. & KALISCH, H. 2025 A novel energy-bounded boussinesq model and a well balanced and stable numerical discretisation. *J. Comput. Phys.* **520**, 113516.
- TUCK, E.O. 2005 Some classical water-wave problems in varying depth. In *Waves On Water of Variable Depth*, pp. 9–20. Springer.
- WHITHAM, G.B. 2011 *Linear and Nonlinear Waves*. John Wiley & Sons.
- XU, J., JIANG, X., FANG, N., GEORGET, E., ABDEDDAIM, R., GEFFRIN, J.-M., FARHAT, M., SABOUROUX, P., ENOCH, S. & GUENNEAU, S. 2015 Molding acoustic, electromagnetic and water waves with a single cloak. *Sci. Rep.* **5** (1), 10678.